PHYS3990 – Semester 1, 2007

Are Magnetic

Storms

Getting Stronger?

Graeme Johnson

7462222

Table of Contents

Are Magnetic Storms Getting Stronger?

Abstract

The aa index has shown an increase over the past 139 years. This result confirms earlier work carried out by other researchers [*Feynman and Crooker*, 1978 and *Cliver et al*, 1998 as cited in *Clilverd et al*, 2002]. The sunspot count data has also shown an increase over the same period of time. Aa data and sunspot data show excellent correlation and so over time sunspot data can be used as a proxy measure for aa. The number of magnetic storms has increased [*Clilverd et al.,* 1998] indicating an increase in solar variability. An increase in solar variability combined with increasing numbers of sunspots would therefore indicate that there would be an increase in strength of magnetic storms. Therefore based on the results and analysis of the data, the strength of magnetic storms does seem to be increasing, however, at a very small rate.

The basis for the investigation into the strength of magnetic storms relates to the effects that space weather in general and geomagnetic storms in particular can have on man-made infrastructure. Space weather can affect spacecraft, aircraft, radio frequency propagation, power generation and transportation systems, oil and gas pipeline systems and humans. There is an ongoing need to develop more robust systems that are exposed to space weather and to better protect the humans that are exposed to space weather. There is also a need to continue developing sophisticated measuring and forecasting systems so that everyone can be prepared for the next big storm.

1. Introduction

Purpose

The aim of this project is to briefly describe the causes of magnetic storms, the subsequent effects of magnetic storms and space weather on ground-based and space-based infrastructure, and whether or not magnetic storms are actually getting stronger, based on current and historical geomagnetic data. It is important to note that some previous researchers have looked at various aspects of geomagnetic data and reported an increasing trend in the aa magnetic activity index over time[*Feynman and Crooker,* 1978 and *Cliver et al,* 1998 as cited in *Clilverd et al,*. 2002]. The main aim here, however, is to examine variations in the aa index over a range of time scales and to also look at the peak intensity of actual storms during this same time period.

The Sun, the IMF and the Magnetosphere

The behaviour of our Sun influences almost everything that we do on and above our planet Earth. It is hard to imagine that events that occur on the Sun can have drastic, even catastrophic, effects upon the Earthand the adjacent surrounding space. The main effects that I wish to discuss here relate to the changes in energetic particle fluxes, and, in the electromagnetic field which originates from the Sun and finds its way to us.

Solar phenomena such as sunspots, coronal mass ejections, coronal holes and solar flares can extend into interplanetary space and have a major impact on the magnetic field which is generated from within our planet. It is the disruption to our magnetic field caused by these phenomena that is a cause for much research, investigation and concern.

To begin the story the Sun has its own magnetic field. Changes in this field can occur in a matter of minutes. A solar flare is defined as a sudden, rapid, and intense variation in brightness. Flares occur when magnetic energy that has built up in the solar atmosphere is suddenly released. Radiation is emitted across virtually the entire electromagnetic spectrum, from radio waves at the long wavelength end, through optical emission to x-rays and gamma rays at the short wavelength end. The amount of energy released is enormous, and all manner of solar material, including a portion of the solar magnetic filed, is flung into space. The same thing occurs with coronal mass ejections. Enormous amounts of matter and energy are hurled into space with the accompanying background magnetic field [*What is a Solar Flare?*, no date=n.d.].

Sunspots, coronal holes and coronal mass ejections are visible manifestations of the solar magnetic field. A sunspot is a dark part of the sun's surface that is cooler than the surrounding area. It is cooler because of a strong magnetic field there that inhibits the transport of heat via convective motion in the Sun. The magnetic field is formed below the sun's surface, and extends out into the sun's corona [*Sunspots: Modern Research*. (n.d.)]. Sunspots always occur in pairs in areas where the magnetic field lines leave the Sun’s ‘surface’ and then re-enter. The presence of sunspots indicates the relative ‘activity’ of the Sun, with low sunspot numbers indicating a quiet Sun and high numbers indicating an active Sun.

The entire structure of the Sun's global magnetic field changes on an approximate 11 year cycle. Every 11 years, the Sun moves through a period of fewer, smaller sunspots, prominences, and flares (called solar minimum) and a period of more, larger sunspots, prominences and flares (called solar maximum). A maximum and a minimum, taken together, make up one solar cycle. During the 11 year cycle, the strongest magnetic fields (in sunspots) slowly migrate towards the Sun's equator from locations about midway to the Sun's poles. They are actually following the field lines generated within the Sun. After 11 years, when the next cycle starts, the magnetic field poles are reversed. Figure 1 shows a ‘butterfly’ diagram which illustrates this migration of sunspots from the mid latitudes toward the solar equator in roughly 11 year cycles. The solar magnetic field therefore has a 22 year cycle while the sunspot cycle is 11years [*The Sun's Magnetic Field Changes*. (n.d.)] .

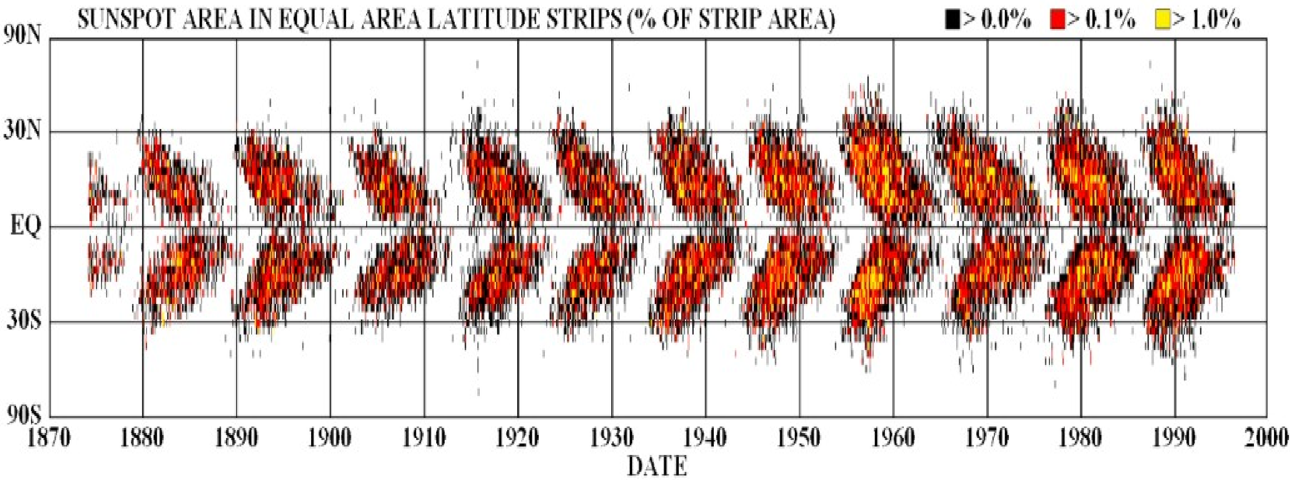

Fig 1: Butterfly Diagram Showing Sunspot Migration with Time. (*Butterfly Diagram*. (n.d.))

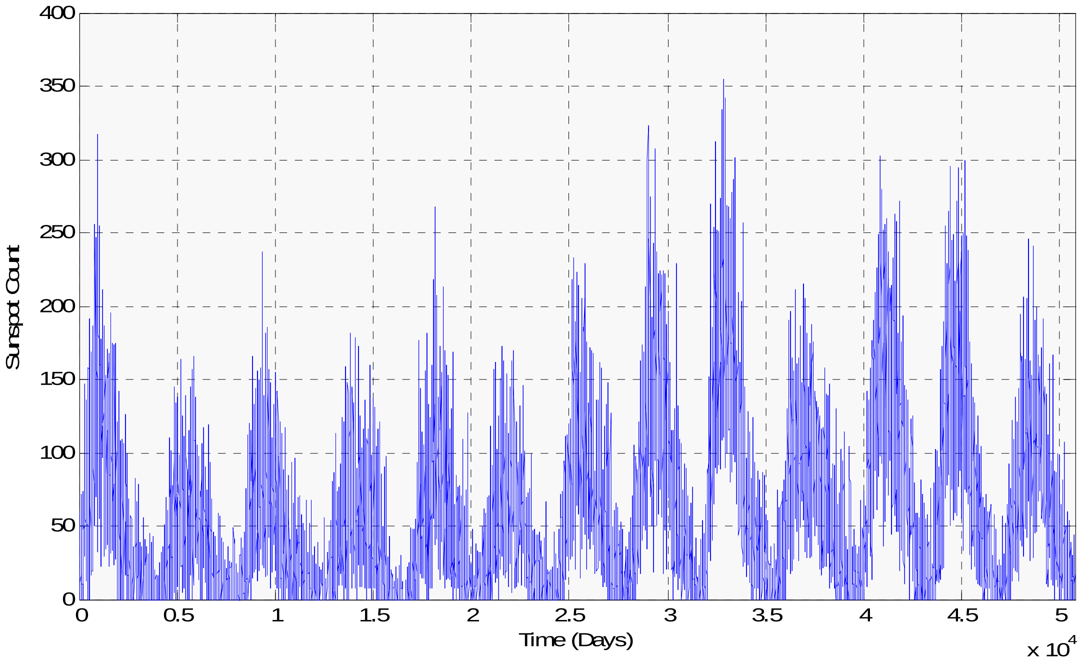

Fig. 2: Plot of Sunspot Count for Period 1.1.1868 to 31.12.2006.

Figure 2 shows a plot of sunspot count for the period 1 January, 1868 to 31 December 2006 using data gathered as part of this project. It can be seen when compared with the butterfly diagram that as the sunspots migrate towards the Sun's equator during the 11 year solar cycle there is also an increase in the number of the sunspots, culminating at solar maximum. At this point the Sun is in a very active state. Figure 3 shows a very large sunspot group that was observed on such an occasion by the MDI instrument on NASA's Solar and Heliospheric Observatory (SOHO) satellite.

Coronal holes, like sunspots, are regions where the corona appears dark. Coronal holes are associated with "open" magnetic field lines and are often found at the Sun's poles. The high-speed solar wind is known to originate within coronal holes [*Coronal Holes*.(n.d.)].

The plasma of ionized particles and magnetic fields that moves outward from the Sun is what is more commonly known as the solar wind, and, the magnetic field that is associated with this solar wind is called the Interplanetary Magnetic Field (IMF) [*Campbell*, 1997].

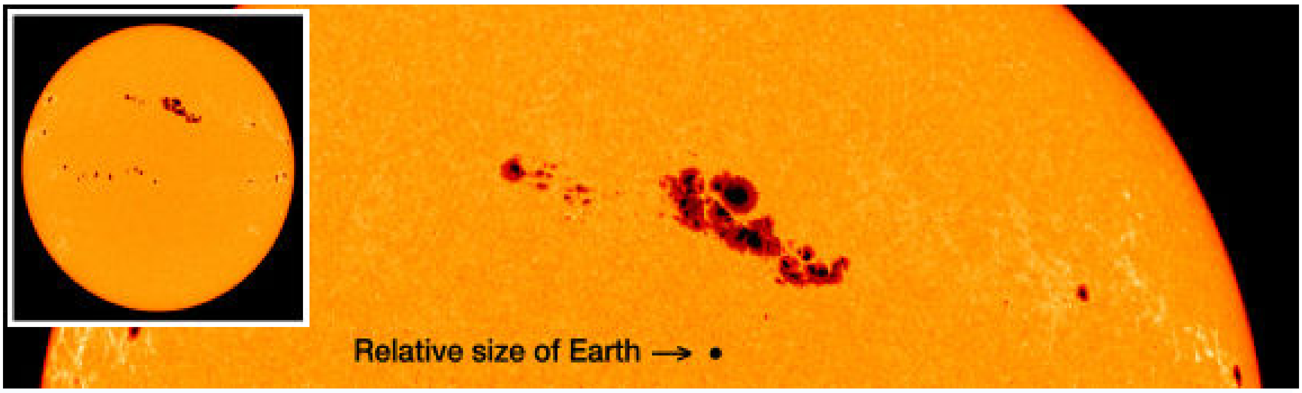

Fig. 3: Active region 9393 as seen by the MDI instrument on NASA's Solar and Heliospheric Observatory (SOHO) satellite. On 30 March 2001, the sunspot area within the group spanned an area more than 13 times the entire surface of the Earth. It was the source of numerous

flares and coronal mass ejections, including one of the largest flares recorded in 25 years on 2 April 2001. (*Sunspot*, 2003).

Energetic particles also originate from the Sun in coronal mass ejections (CMEs). These are apparently not necessarily related to solar flares but did include a range of disturbance phenomena associated with closed magnetic field lines within the corona. CMEs are more broadly spaced across the Sun's surface than are flares, which seem to be found only in lower latitudes.

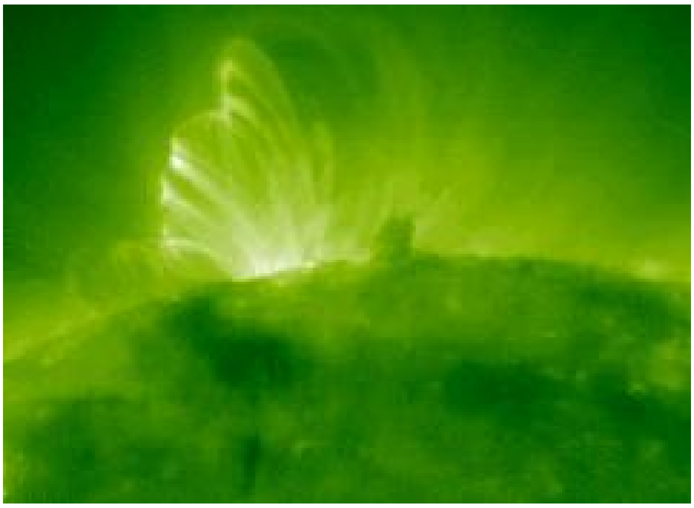

Fig. 4: Image of Coronal Loops taken by satellite Yohkoh (*Coronal Features* (2007)).

CMEs are believed to be responsible for populating the solar wind with protons, electrons and heavy ions when they eject matter into space. Figure 4 shows a large coronal loop shooting matter into space.

The solar wind has a typical velocity of order 400 km/s. The combined motion of the solar wind particles in the magnetic field actually drags along the field itself. The solar wind has an extremely high electrical conductivity (approximately 10^4 Siemens/meter) and can be regarded as a virtually perfect conductor. Such a conductor moving within a magnetic field generates currents that hold the internal magnetic field constant within the conductor. A sample of solar wind will therefore change with time but it will still hold the original magnetic flux. This is what is called a frozen-in field [*Campbell*, 1997].

Active events on the Sun can affect the amount of material entering the solar wind and also its velocity which can increase to well over 1000km/s. This results in shockwaves within the solar wind. The shockwaves are caused by fast moving solar wind created by the solar event, compressing slower moving solar wind in front of it. The interaction of these shockwaves with the frozen-in magnetic field can cause serious geomagnetic events in the Earth's magnetosphere. Depending on the orientation of the IMF and the intensity of the associated charged particles within the solar wind, a geomagnetic storm will be generated [*Campbell*, 1997]. Figure 5 is a schematic representation of the Earth's magnetosphere showing the important constituent regions.

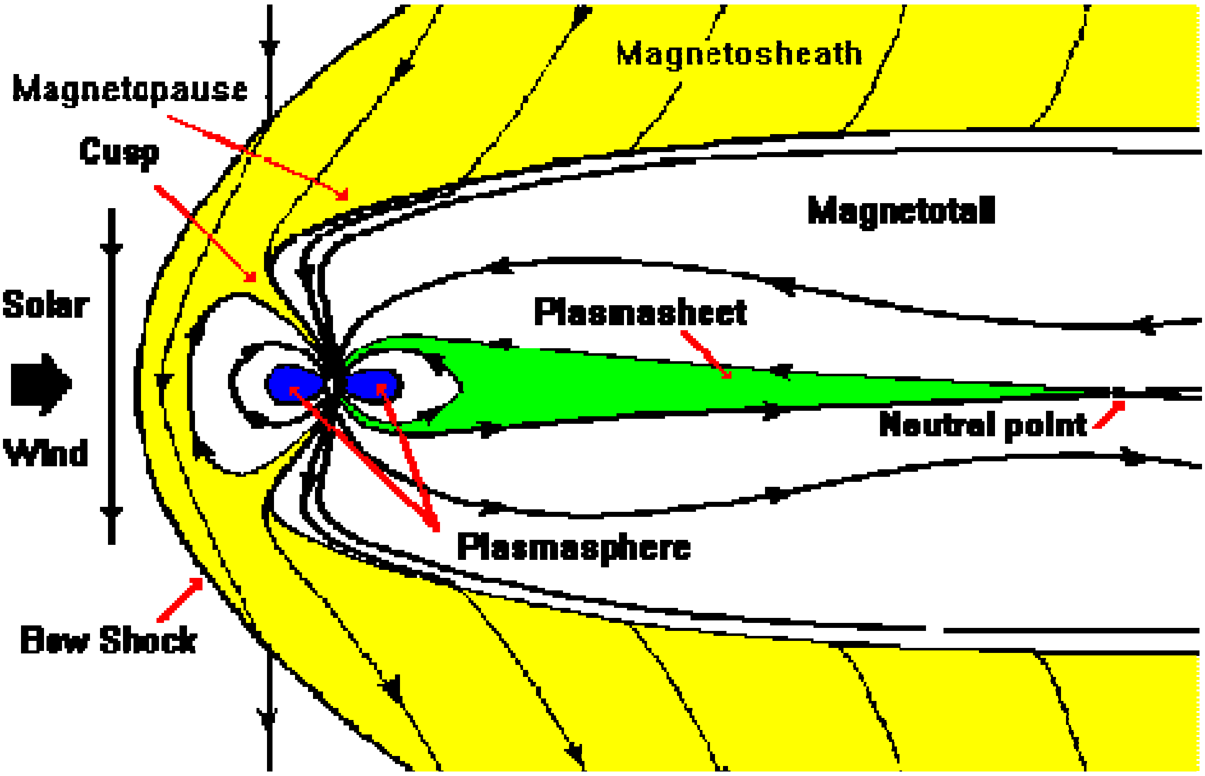

Fig.5: Schematic Representation of the Earth's Magnetosphere. (Courtesy NASA)

The next section will tie in this background information on solar wind – magnetosphere interactions with the basics of magnetic storm generation and their effects on space weather.

2. Magnetic Storms and Space Weather

What are Magnetic Storms?

The major factor in the generation of geomagnetic storms is the orientation in space of the interplanetary magnetic field (IMF). At the nose of the magnetosphere a southward directed ($-B_z$) component of the IMF encounters the northward-directed magnetic field of the Earth. The field lines then interconnect and in doing so allow entry for the solar-wind particles into the magnetosphere. Thus a southward turning of the IMF is the major contributing factor to magnetic disturbances on Earth. [*Campbell*, 1997]

In order to describe the Earth's magnetic field observers have devised two coordinate systems. The first uses a system based on Cartesian coordinates with three orthogonal components. The values are designated X, Y and Z with the positive values being northward, eastward and vertical down. Minus values are given for the other directions. The other system is derived from this but is described as H (horizontal), D (declination) and Z (into the Earth). The H and D components are derived from X and Y in the XYZ system, while Z remains the same Z as before. [*Campbell*, 1997]

The resultant geomagnetic disturbances are called geomagnetic storms, a term which is generally shortened to magnetic storms. There are usually four phases to a magnetic storm, these being the sudden commencement (SC), the initial phase, the main phase and the recovery phase.

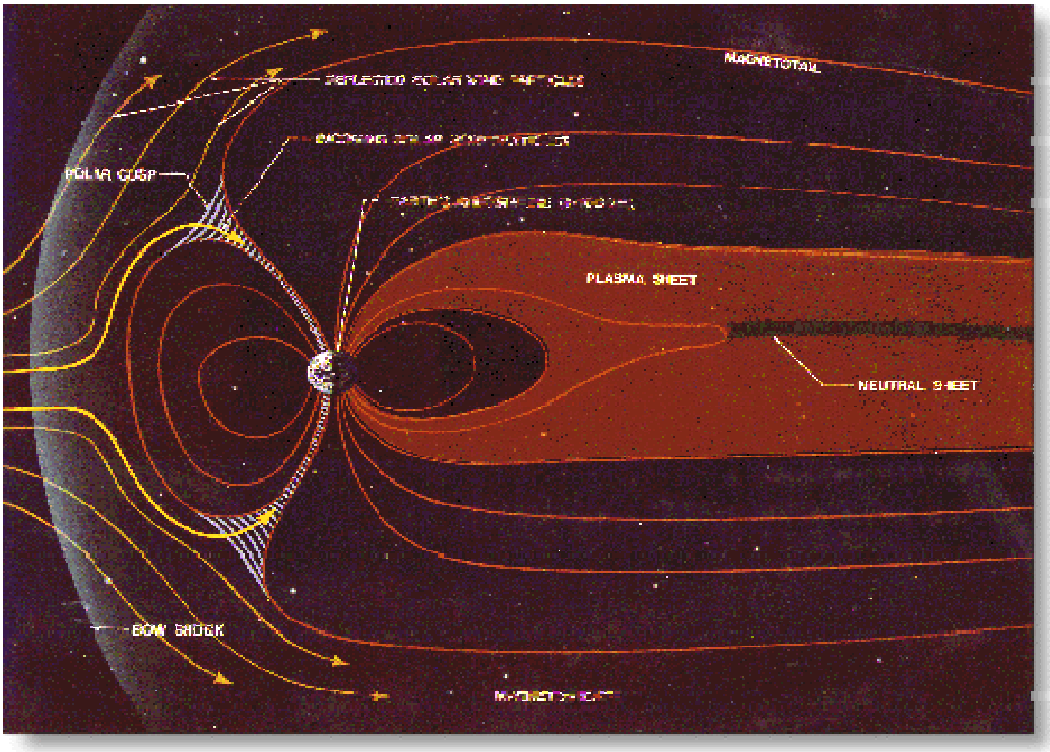

Fig. 6: Schematic Diagram of the Earth's Magnetosphere. (Magnetosphere, nd)

The SC phase is caused by the arrival of a solar wind plasma shockwave at the magnetosphere. This occurs almost simultaneously everywhere across the dayside of the magnetosphere. If the IMF accompanying this disturbance has a southward inclination then a magnetic storm will generally occur. If, on the other hand, the IMF has a northward direction, then there will be no subsequent storm. When this occurs the resultant phenomenon is a sudden impulse.

The next phase is called the initial phase and many storms actually occur without this phase. If present it is marked by an increase in the northward field generally only for a few hours after the SC event.

The main phase of the magnetic storm is the next phase and is characterized by a relatively rapid decrease in the principal component of the field. This phase depends upon a consistent southward directed IMF at the magnetospheric boundary. The main phase will generally last for several hours depending on the size of the disturbance caused by the solar wind. At this point there is also a large injection of ions and other charged particles from the solar wind into the Earth's magnetic field region. These charged particles, with the magnetic field, cause currents to be generated. This current is called the storm time ring current (because it encircles the Earth) and it is the variations in magnetic field caused by this current that can be detected by ground-based observatories. The transfer of energy from these currents between the magnetosphere and the ionosphere cause auroras and other ionospheric disturbances. [*Campbell*, 1997]

The last phase of the storm is the recovery phase. This phase can take from hours to days and is essentially the switching off of the southward IMF and a refilling of the magnetosphere with particles from the atmosphere.

Figure 7 shows a plot of the hourly Dst index (a magnetic disturbance index; see section 3) versus time in hours of the Halloween Storm of 2003. The SC and initial phases are hard to separate however the main phase (strong Dst decrease) and recovery phase (gradual recovery of Dst to its previous value) are clearly visible. The other notable feature is the ‘double dip’ in the centre of the plot. This was caused by the initial disturbance, closely followed by a second equally powerful disturbance to the magnetic field. This was a notable storm and it will be discussed in more detail later.

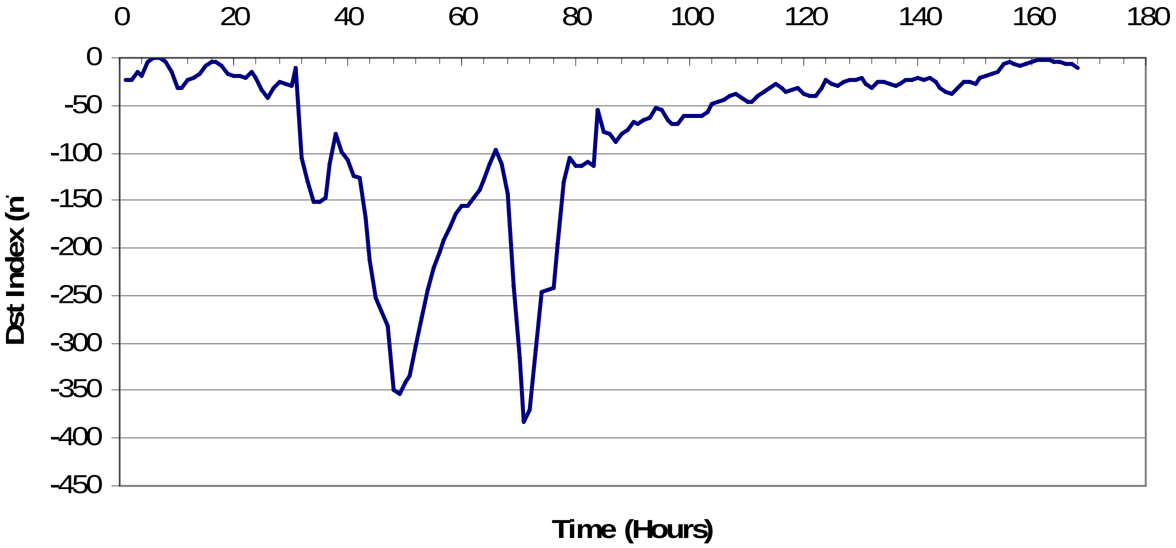

Fig. 7: Plot of Hourly Dst Index (nT) and Time (Hours) for Period 28.10.2003 to 3.11.2003 (Halloween Storm of 2003)

There are two types of geomagnetic storm; recurrent storms and non-recurrent storms. The recurrent storms occur approximately every 27 days and are linked to the rotation period of the Sun. These storms occur more frequently during the declining phase of the solar cycle. Non-recurrent storms are caused by singular solar events such as coronal mass ejections (CMEs) and solar flares which greatly disturb the IMF and so cause the changes in the magnetosphere that would trigger a magnetic storm. [*Geomagnetic Storm.* 2007]

Space Weather and Its Effects

The term space weather refers to the time-variable conditions in the space environment that may affect space-borne or ground-based technological systems and, in a worst-case scenario, endanger human health or life. The most important social and economic aspects of space weather are related to being aware of and possibly avoiding the consequences of space weather events either by system design or by efficient warning and prediction systems allowing for preventative measures to be taken [*Koskinen et al*., 2001].

The effects of space weather are many and varied. Effects can include electronic failures in spacecraft and aircraft, immediate and long term effects on astronauts and aircraft crews, interruptions to telecommunication and navigation systems, effects on large metallic infrastructure items such as oil and gas transmission systems and electric power transmission systems. There have also been some reports that space weather may affect the Earth’s climate. With the increased development that is occurring around the world and the manufacture of smaller and more sensitive electronic devices the need to be able to forecast or even nowcast space weather events is of the utmost importance. The above list covers an impressive array of infrastructure worth many billions of dollars. For example, over 900 satellites worth around US$200B to replace operate in Earth orbit.

The insurance industry is therefore another player in space weather game and that could have ramifications for us all.

According to the Space Weather Effects Catalogue [*Koskinen et al*, 2001] several components that make up the space environment produce varying effects on terrestrial and space-borne infrastructure. It is beyond the scope of this current work to detail all these phenomena so only those effects primarily generated by intense solar events and their interaction with our own magnetosphere will be briefly discussed here. These include but are not limited to such things as solar energetic particles, neutrons ejected by the Sun, photons (from γ rays to radio waves) and the solar wind, consisting of plasma and the frozen-in magnetic field. The other main component in this interaction is the Earth's magnetosphere.

Effects on Spacecraft

Most of the components mentioned above can and do affect spacecraft. The importance of the interaction will generally depend on the energy concerned and on the location of the spacecraft in the space environment. Some of the more typical effects are as follows.

- High energy particles can cause atom displacements within solar cells and this can cause permanent damage to the cell. All solar cells therefore degrade in space.
- The direct impact of high energy protons or heavy ions can cause background noise problems in photon detectors.
- Charging effects caused by electrons and other particles being deposited on the outside of the spacecraft and then the charge making its way to sensitive instrumentation or guidance systems. All spacecraft experience charging effects, and mitigating these is a major engineering challenge.
- Single Event Effects (SEEs) such as single hard errors, single event upsets, latchups, burnouts, gate and dielectric ruptures, in electronic devices. As these events are caused by a single particle that particle must have enough energy to pass through the shielding of the spacecraft before striking the electronic device. Particles with energy > 10 MeV are able to do this and so high energy protons and heavy ions are the primary cause of SEEs.

It has not been uncommon for blasts of high energy radiation to have disabled satellite systems. Particular events such as the Halloween Storm of 2003 disabled numerous satellites and seriously affected many more.

The effects noted above relate to space hardware. However, on manned space flights even though there is extra shielding, the human cargo can still be susceptible to external radiation effects. During so called Solar Energetic Particle Events (SEPEs) astronauts must move to specially shielded areas of their spacecraft. The US Space Shuttle fleet and the International Space Station have special 'safe' areas where crew can go if there is a SEPE. Any extra vehicular activity (EVA) is then curtailed as the potential risks can be lethal [*Koskinen et al*, 2001].

Effects on Aircraft, Crew and Avionics

Similar problems can arise with aircraft, aircrew and avionics systems. Electronics are susceptible to SEEs and aircrews are susceptible to high energy particles at higher altitudes. Although the most energetic incoming particles are cosmic rays, which do not originate from the Sun, during periods of high solar activity other high energy particles can and do cause damage. Restrictions are placed on aircrew traveling great circle polar routes, as at the poles there are open magnetic field lines and radiation can more easily enter the Earth's atmosphere.

To increase awareness of the problem that radiation can cause to the health of both aircrew and passengers, the European Union issued Council Directive 96/29/EURATOM to take effect in May 2000. Article 42 of this directive demands that aircraft operators must take account of the exposure of their crew to more than 1 mSv (milliSievert) per year of ionizing radiation. Mitigation strategies involve redeploying aircrew or moving flights to lower altitudes during active solar conditions. [*Koskinen et al*, 2001]

The effects of SEEs on electronic equipment are increasing as these electronic components and instruments get smaller and lighter (i.e. with less shielding). The radiation hazard for aircraft at normal operating altitudes of 9 km (30000 ft) can be as high as spacecraft in low Earth orbit. The problem here is not damage from primary radiation as this is predominantly shielded by Earth’s atmosphere. It is caused by a build up of secondary radiation (neutrons, mesons, electrons) in the near Earth environment. These are at a maximum at approximately 18 km (60000 ft). This radiation causes indirect ionization by nuclear reactions in the electronic material [*Koskinen et al*, 2001].

Effects on RF (Radio Frequency) Propagation

The ionosphere is a region of the Earth’s atmosphere that extends from 80 to over 400km altitude. This area of the atmosphere is partially ionized and thus can greatly affect the propagation of radio frequency signals. The systems that can be adversely affected by events in the ionosphere include:

- Ground-ground high frequency (HF) communications
- Ground-space communications
- Global Positioning System (GPS) – particularly single frequency - navigation systems
- High frequency (HF) over the horizon radar systems
- Satellite altimeters
- Space-based radars.

The majority of these systems rely on the ionosphere for propagation of their respective signals, however they must also contend with the effects of its dynamic nature [*Koskinen et al*, 2001].

Effects on Ground Based Power Systems

The induction of electric currents in electric power grid systems during periods of severe geomagnetic activity is well documented. The effects can vary from the tripping of circuit breakers, which may cause temporary loss of power; to the destruction of power station transformer banks which are very expensive and cause longer term power shortages. These larger catastrophic events also cause huge economic loss to both private and industrial users. The problem here is that magnetic storm induced currents find their way to the three-phase transformer systems that are connected to the power grid. These currents cause intense localized heating within the transformers causing capacitors to become overloaded and protective relays to trip out. The transmission of power is then restricted or lost completely. These problems are greatest in high latitude countries (Scandinavia, Canada, etc). [*Campbell*, 1997]

Examples of serious failures include:

- On 4.8.1972, a Kp 9_0 magnetic storm caused the failure of a 230 kV transformer at the British Columbia Hydro and Power Authority of Canada.
- On 13.4.1989, a Kp 9_+ magnetic storm caused a nine hour blackout of the 21000 MW Hydro Quebec power system.

- The same 1989 storm destroyed transformers at the Salem Nuclear Plant (US) of the Public Service Electric and Gas Company, with a replacement cost of $12 million (US).

Based on these experiences electricity generation companies are employing redesign and failsafe systems in an attempt to prevent any of these sorts of failures happening again [*Campbell*, 1997].

Effects on Pipelines

Oil and gas pipelines are also prone to the effects of space weather. Most oil and gas pipelines have protective coatings applied to their external surface. This is always the case when the pipeline is buried in the ground. However if this external coating is damaged then corrosion can occur where exposed metal comes in contact with the surrounding earth. To avoid rapid deterioration of the pipeline due to this type of corrosion, cathodic systems are put in place to reduce the potential difference between the pipeline and the earth. During magnetic storms the current induced into pipelines can be high (due to the relatively large, varying currents in space) and it is this sudden increase in current that can affect the potential difference between the pipe and the soil. The damage is caused through large potential differences damaging the cathodic protection systems on the pipeline. The induced current itself doesn't cause the damage it is the effect of having no protection that can possibly increase corrosion rates [*Koskinen et al.,* 2001, p22]. In August 2006 BP closed pipelines to the Prudhoe Bay oilfield in Alaska after discovering 'unexpectedly severe corrosion' and 'corrosion related wall thinning' [www.bp.com], cutting 8% of US oil production.

Summary

Space weather effects can have a large impact on a wide variety of infrastructure. The importance of knowing when an event will occur is paramount. This is the reason why there is widespread research into space weather effects and how to minimize their effect. The other reason is for the likes of insurance companies who are insuring trillions of dollars worth of infrastructure against possible damage or destruction.

3. Indices and Measurements

The Geomagnetic Indices. [*Menvielle,* 1998]

From the Earth's surface it is possible to measure and observe features of various magnetospheric phenomena such as visible aurorae, changes in ionospheric parameters and variations of the Earth's magnetic field. Over many years data bases of various indices have been built up giving researchers large data sets on which to perform analysis of these phenomena. Some of these data sets cover extensive periods of time (e.g. aa data covers about 140 years) and also span various parts of the planet. In this project we focus on geomagnetic indices that indicate the state of disturbance of the geomagnetic field. Since these indices provide a continuous monitor of magnetic variations within the ionosphere and magnetosphere, they form the basic data in any space weather research.

When looking at these indices and the variations they represent, it is important to separate them into two categories, a regular component and an irregular component.

Regular Variations

The main source of regular variation is ionospheric tidal currents generated by the heating and ionization of the dayside atmosphere. These variations are present during quiet and disturbed times, but regular variations have a smooth shape and a regular occurrence. The individual solar regular variation is designated as S_R [Mayaud, 1965] and S_q is the variation deduced from the S_R data by averaging them over a given time interval. Sq thus represents the systematic diurnal, monthly and seasonal variation in the geomagnetic field.

Irregular Variations.

These variations are mostly due to the energy input in the magnetosphere from the disturbed Sun. They relate to magnetospheric storms. A point to note is that when terms such as magnetically quiet or disturbed are used, they refer only to irregular variations. Typically irregular variations have time scales of minutes to hours, although longer periods can be associated with high energy events in the magnetosphere. The intensity of irregular variations varies considerably with latitude. The largest variations are generally seen at latitudes between 60 and 70 degrees. These latitudes correspond with the auroral zone. The amplitudes of the irregular variations range from a few nanoTeslas (nT) to many hundreds of nT. The third important aspect of irregular variations is that their latitudinal extension depends on the time period and this is associated with exposure to the day side or night side magnetosphere.

Definition of Indices

Indices are intended to describe defined phenomena from a particular set of measurements [Menvielle, 1998]. He states that there are two complementary viewpoints. One starts from a given phenomenon and then describes a measurement method to derive an index. The other starts by analysing available measurements of the physical quantity, and then describing the phenomena that go with it.

With geomagnetic indices, the second standpoint was adopted. The measured physical quantities are the perturbations in the magnetic field recorded at a number of observatories around the Earth. From analysis of these perturbations it was found that they reflect distinct phenomena of ionospheric and magnetospheric origin. More precise indices were established in order to describe specific magnetospheric phenomena.

The International Association of Geomagnetism and Aeronomy (IAGA) has developed a range of such indices. These are derived in terms of four main parts:

- The quantity to be measured
- The measurement time interval
- The location of the station or network of stations
- The method of deriving the index

A brief description of each of the current main indices follows.

The Auroral Activity Indices. (AE, AU, AL).

The auroral activity indices measure the deviation of the horizontal component of the geomagnetic field from a base reference value. The indices are measured in units of nT and are available from 1957 onward. The measured values have one minute resolution since 1978. Readings are taken from a network of stations in the northern auroral zone.

The Equatorial Dst Index.

This index also measures the deviation of the horizontal component of the geomagnetic field from a base line determined from secular variation. The readings are taken hourly from a network of four stations located at low latitudes around the Earth. The resulting index is a measure of the disturbance in the geomagnetic field resulting mostly from effect of the magnetospheric current, measured in nT.

The K Indices.

These indices measure the amplitude of the irregular variations, on a relative scale. Readings are taken at 3 hourly intervals starting at 00:00 UT each day at each standard magnetic observatory around the globe. Although the K indices are thus defined everywhere they are largest at auroral and sub auroral latitudes.

The Kp, ap and Ap Indices.

These indices have been measured since 1932. They are obtained from the average of 11 northern and 2 southern hemisphere stations and represent the global level of geomagnetic variation during each 3 hourly interval. K values for each individual station are converted into standardised indices 3Ks. 3Kp is the sum of the 3Ks values divided by 12. The 3Ks and 3Kp values are integers in the range 0 to 27. Kp values are given as 0o, 0+, 1- to 9o. A further parameter, ap, is then defined as the disturbance value in units of 2nT obtained from Kp through a conversion table, and Ap is further the daily average of ap.

The an, am, as, Kn, Km, Ks, An, Am and As Indices.

These indices have been measured since 1959. The values are range amplitudes deduced from K indices. These indices are measured three hourly at a network of 13 northern and 10 southern subauroral stations arranged in groups representing longitude sectors. For each of these longitude sectors, averages of K are converted into range amplitudes and corrected for differences in the extent in longitude. an is the average for the northern stations and as is the average for the southern stations, both measured in nT. The am index is the average of the an and as indices i.e. am= (an + as)/2. Kn, Ks, Km are K values obtained from the an, as and am values using a conversion table. An, As and Am are the daily averages of an, as, and am.

The aa Indices.

These indices are the longest running geomagnetic indices and have been recorded since 1868. Like most of the other indices, the aa index comprises range amplitudes deduced from K indices. They are calculated on a three hourly basis and then averaged daily. The measurements for this index are taken at two antipodal, sub auroral observatories, one in England and the other in Australia. The actual observatories have changed over the years and commenced at Greenwich (1868-1926) and Melbourne (1868-1926). The Greenwich Observatory was superseded by Abinger Observatory (1926-1957) and then Hartland Observatory (1957- present). Similarly in the southern hemisphere the observatory at Melbourne was superseded by Toolangi (1926-1980) and then an observatory just outside of Canberra (1980 – present) [Clilverd et al., 1998].

The aa index expresses geomagnetic variation amplitudes deduced from K that are corrected for small variations in the latitudes of the two observatories. It is an average of the two amplitude values determined in England and Australia. The Aa value is the daily average of the aa value. Both aa and Aa are measured in units of nT.

Measurement of Geomagnetic Indices.

The presence of a magnetic field is not an obvious phenomenon. It is not like wind or rain which can be seen and felt with normal human senses. In order to measure a magnetic field we need to observe the interaction of that field with other physical phenomena and from the point of view of measuring geomagnetic indices there are a number of factors that need to be taken note of.

The first point is that the Earth's magnetic field is ever present. It doesn't get switched off. We need to take calculated and premeditated action to prepare a magnetic field free environment. The large number of geomagnetic observatories located around the world have all been carefully located within their communities and then very carefully built so as to reduce the effects of 'noise' from the local environment. This noise could be created from metallic infrastructure such as buildings, bridges, pipelines, electricity transmission lines and transformers, motor vehicles, etc.

The next point to note is that spatial size of this omnipresent magnetic field will generally only allow single point measurements to be taken. This factor then requires that a number of observatories are spread over the surface of the Earth and also in space. The field itself is also made up of several components and each of these makes a contribution to the overall measurement being taken. In order to determine the magnitude and direction of the vector component it is important to know form of the normal steady state field and then make allowances for this when taking measurements. [*Campbell*, 1997]

The steady field is a very strong, slowly changing field when compared to some of the minute fields caused by rapid external pulsations. Detection instrumentation therefore needs to be designed to accommodate a large dynamic range, from 10^{-3} to 10^{5} nT, or alternatively the detection apparatus must be limited to a very narrow band of a specific geomagnetic index. There have been a number of different types of measuring devices that have been used to measure the Earth's magnetic field over time and I will briefly discuss some of the more historically significant of these. The term used for a device that measures the magnitude of a magnetic field is a magnetometer, and depending on the type used it can measure both the magnitude and the direction vector of that field. [*Campbell*, 1997]

The observatories at Hartland, UK and Canberra, Australia, which are the observatories used to derive the aa index, both employ fluxgate magnetometers to measure the H, D and Z components of the field. These observatories also have proton precession magnetometers to measure the total field which are thus used to calibrate the resident fluxgate devices. [*Hartland Observatory Monthly Magnetic Bulletin*, 2007; *Australian Geomagnetism Report*, 1999].

The Variometer.

The first variometer was developed in the late 18th century when researchers used long compass needles to measure the effects of magnetic storms. In 1840, Gauss improved on the original design by affixing mirrors to the compass magnet suspension. By tracking a light beam reflected from a mirror, he was able to measure the deflection of the compass very accurately. The development of photographic techniques in the late 19th century allowed automatic measurement of the time rate of change.

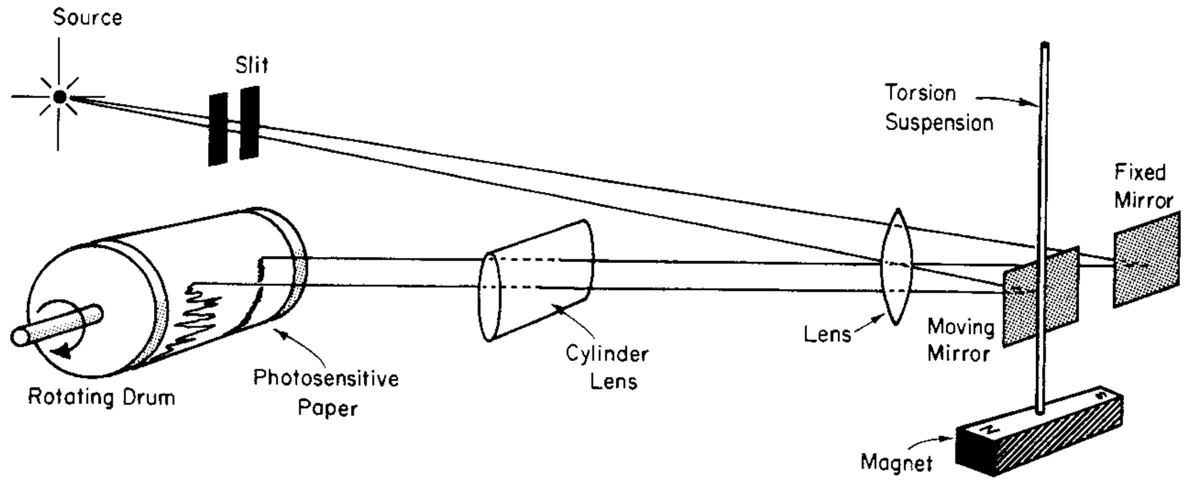

Fig. 8: Schematic Diagram of Variometer Type Magnetometer. (*Campbell,* 1997. Fig 4.3)

Figure 8 shows a schematic representation of a variometer. The magnet is suspended in such a way as to be able to resolve the H, D or Z components of the magnetic field and it is zeroed appropriately. A light beam is reflected off the mirror system onto a moving roll of photographic paper. As can be seen in the diagram the output from the mirror attached to the magnet is compared to that of a fixed mirror and the difference is the change in the appropriate component being measured. Some observatories converted the analogue systems to electronic systems by using calibrated photometers to measure the variations in light received.

Variometers being mechanical devices are prone to temperature and humidity effects as well as physical vibrations. It is important to house variometers in a well designed building that reduces these effects. There is also the problem of fatigue in the suspension system. Variometers have been widely used around the world and in some cases are still used. Their proven reliability, low cost and simplicity is the major factor in their use. Fairly recently, however, more advanced devices have taken the place of the variometer in the main geomagnetic observatories.

The Fluxgate (Saturable-Core) Magnetometer.

Fluxgate magnetometers are now widely used as the magnetometer of choice in most of the main geomagnetic index measuring observatories. The operation of this type of magnetometer is based on the nonlinearity of the magnetization properties of easily saturated ferromagnetic alloys, this being used as an indicator of magnetic field strength. The term fluxgate used here refers to periodic switching of magnetic flux in the detector.

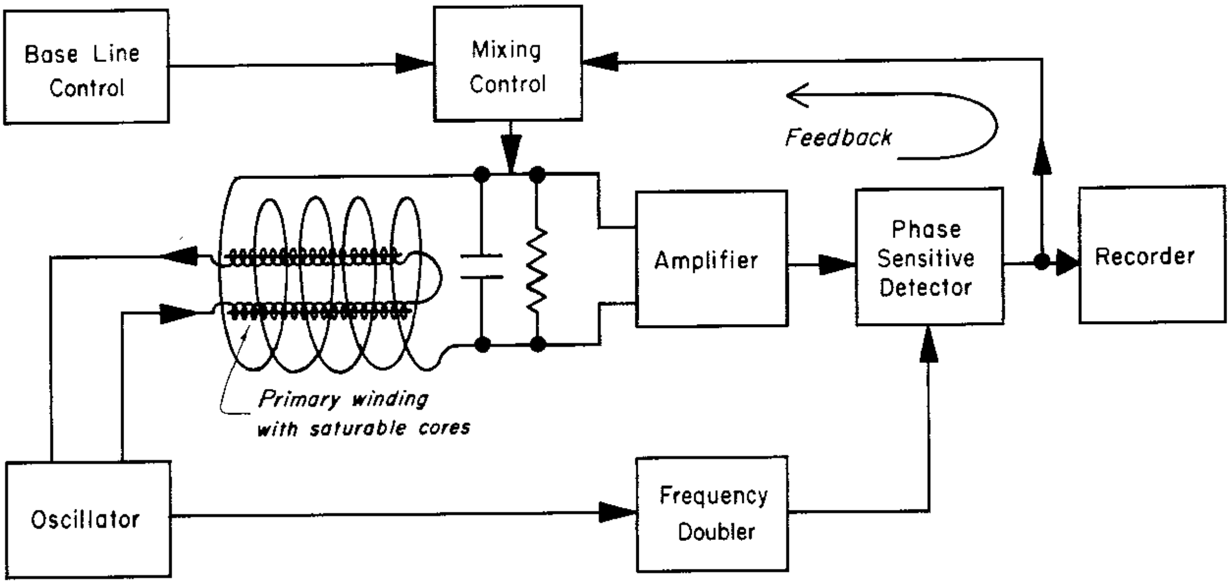

Fig. 9: Schematic Diagram of Fluxgate Magnetometer for Directional (Vector) Geomagnetic Field Measurement. (*Campbell,* 1997. Fig 4.9)

This type of magnetometer uses a high permeability magnetic material to amplify the magnetic field signal picked up in a tiny loop antenna system. The hysteresis properties of the core material are exploited by using a strong oscillating field. This field is offset by the natural local field. The strength of the geomagnetic field is obtained from the generation of distortion harmonics in the output field, measured by secondary loops around the core. In the more common version of this type of magnetometer the quantity measured is the second harmonic component of the excitation frequency. Figure 9 shows a schematic representation of a fluxgate magnetometer. These magnetometers are chosen when electronic registration of the field is needed. They are reliable and robust, being used at most modern geomagnetic observatories and also in many satellites. Two problems are that these magnetometers are temperature sensitive, and the need for absolute calibration. This problem has been solved at most observatories by using a proton-precession magnetometer reference.

Proton Precession Magnetometer.

A proton is a hydrogen atom stripped of its electron. In a hydrogen-rich liquid, the protons are not tied to a crystal lattice. The proton can be considered a spinning charged sphere having an inherent magnetic moment, m_p, and an intrinsic spin angular momentum, I_p. The ratio of these two vectors is a scalar called the gyromagnetic ratio, γ_p. In the presence of an external magnetic field a torque will be exerted on the spinning proton to align its magnetic moment. This causes the proton spin axis to precess. The proton’s spin angular velocity is an atomic constant and it is the force of the magnetic field that changes. The angular frequency of the proton precession, ω_p, is called the Lamor frequency. The Lamor frequency is equal to the product of the gyromagnetic ratio and the magnitude of the total field. Therefore if we know the gyromagnetic ratio, we can determine the local total field strength by measuring the frequency of the proton precession.

The protons need to be orientated correctly for these measurements to take place and so they are subjected to a strong magnetic field at an angle to the local field. If the polarizing field is then reduced the protons will precess about the external field and induce a signal in the pickup coil. Usually these are one in the same coil. Figure 10 shows a schematic representation of a Proton magnetometer. In the diagram the coil around the proton sample is used to both align the protons and detect the proton precessional period.

Liquids such as water, alcohols, oils, and kerosene have been used as a proton source. Sensitivity is limited by the ability to accurately determine the gyromagnetic ratio, the duration of the signal, the integration time of the frequency counter and the field gradient across the sample. This type of magnetometer is used in observatory situations as a calibration unit for the fluxgate magnetometers.

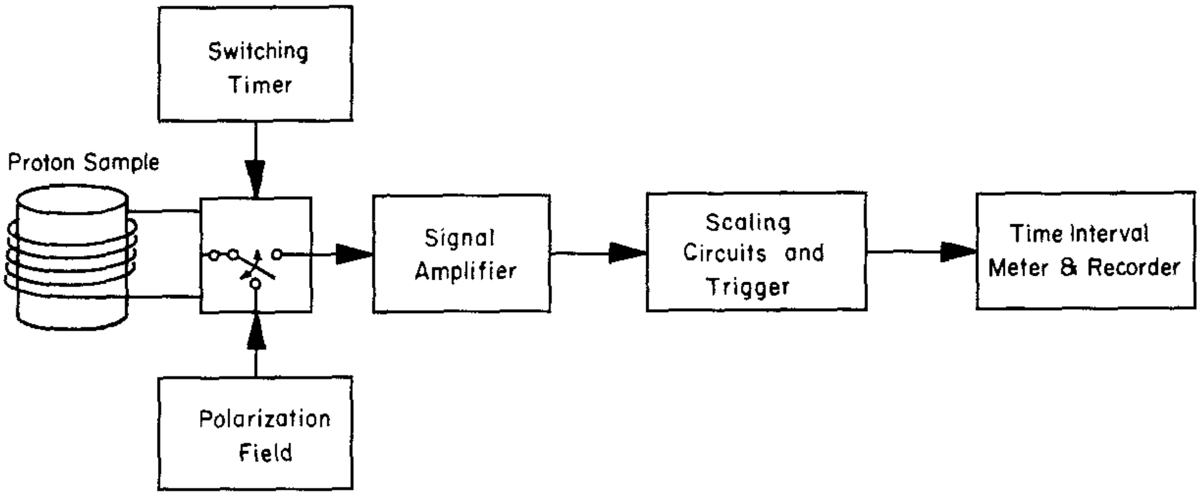

Fig. 10: Proton Magnetometer for Total Field (Scalar) Geomagnetic Field Measurements. (*Campbell*, 1997. Fig 4.11)

Measurement of Magnetic Storms.

Any of the indices mentioned above can be used to monitor the development of a magnetic storm. The primary index for representing the phases and the intensity of a magnetic storm is the Dst Index. The location of the four low latitude observatories enables them to measure variations in the H component of the magnetic field which relate to the development of the ring current as a storm progresses from initial through to main and recovery phases.

The other indices that are widely used to measure the magnitude of geomagnetic storms are the aa and Aa indices. These are the longest continuously recorded indices and it is possible to use these indices to determine the occurrence and intensity of geomagnetic storms. These indices are calculated from a K index on a three hourly basis and then averaged daily. It is possible to look at the individual readings (aa) to determine the greatest magnitude of any storm in question. This was not done here due to time constraints. The daily average values (Aa) were used. These still provide an excellent method for determining storm intensity.

While doing researching for this project it was found that there was no clear criterion for determining what value of aa or Aa constitutes the benchmark for defining the occurrence of a geomagnetic storm. Clilverd et al [2002] state that they had used a threshold value of 40 nT to indicate the commencement of a storm, which was deemed to have ended when the aa value dropped below 40 nT for two consecutive 3-hour periods. This value appears to be an arbitrary one but for the purposes of this project it was also taken to be the case. Appendix 1 is a copy of the NOAA Space Weather Scale for Geomagnetic Storms which gives an indication of the severity of geomagnetic storms using the Kp index [*NOAA Space Weather Scale for Geomagnetic Storms* (2005)].

4. Method

In order to answer the question, ‘Are Magnetic Storms Getting Stronger?’ it was important to determine what type of data would provide the best results. With the number of available indices it was necessary to determine which one would give the best indication of both averaged trends over time, and trends when considering the intensity of individual storms over the years of data. The Aa index was chosen because it is derived from the longest running continuous data set of geomagnetic data, the aa index. The aa index was retrospectively recalculated back to1 January, 1868 by Mayaud in 1972 and so the aa index therefore gives a continuous data set covering approximately 139 years. It has also been checked by a number of researchers for accuracy by comparing the aa figures from the antipodean locations with suitably calculated values of aa from various other observatories [Clilverd et al., 2005]. There have also been checks made to ensure that there are no instrumental errors caused by moving the aa measurements to different observatories during the 139 year history of aa measurements. This has only been done for the northern hemisphere observatories and the variation was found to be of the order of 2nT [Clilverd et al., 2002].

The data set for aa and Aa was accessed via the world wide web from the International Service of Geomagnetic Indices website. In essence, all geomagnetic data are housed in international repositories called World Data Centres. The data were organized on this website in monthly blocks of 3 hourly aa readings, along with the daily average value of Aa. The 3 hourly Kpa index was also included for each day.

This data set was meticulously cut and pasted into an Excel spreadsheet so that the required segments of data could be sorted and then analysed. This was the crux of the exercise so extreme care was taken to ensure that all the data were collected and no mistakes were made during the collection process. Several checks were made to ensure data integrity. The data used for the exercise comprises Aa values for each day from 1 January, 1868 to 31 December, 2006. This is therefore a data set containing 50,769 data points. It was anticipated that since this was such a large data set taken over a significant period of time, that there would be enough data points to give an indication either way to the question at hand.
The other data that was used in this project was daily and annual average sunspot counts. This information was found on the National Geophysical Data Centre (NGDC-US) website. The National Oceanographic and Atmospheric Administration is the agency responsible for the data and because it is a US government agency, the data it collects and distributes is not subject to copyright.

The sunspot count has been recorded continuously for a very long period of time, centuries in fact. The time period that needed to be covered by the geomagnetic data can also be covered by the available sunspot data. It was also possible to go back further in time with the sunspot data to see if it was possible to determine if the sunspot data could be used as a proxy measure for the aa index. In a similar fashion to the aa data, the sunspot data were collected and put into an Excel spreadsheet so that it could be further manipulated. Once both sets of data had been collected they were transferred to Maple so that further analysis could be carried out. The reason for this was that Excel has a limit on the number of data points that can be plotted from one worksheet and this data set was too large for Excel.

It was decided that to best evaluate the data there should be a number of plots that would identify trends and would possibly determine if magnetic storms have been getting stronger over time. The first plots that were produced show the raw data. For Aa and the sunspot count this is a plot of the daily readings plotted against time. With these plots linear tend lines were fitted in an attempt to identify any trends that may be present.

It was then decided to produce a yearly average plot of both Aa and sunspot count. It was envisaged that this would tidy up the data by eliminating noise created by the large numbers of data points in the raw data set. With these plots trend lines were also included; a linear trend line and a cubic trend line. The notion here was to identify long-term trends.

The next set of plots were log-log plots of a fast Fourier transform (FFT) analysis of both the Aa and sunspot count raw data. The FFT is used for spectral analysis of discrete data sets. It takes a discrete signal in the time domain and transforms that signal into its discrete frequency domain representation. This process was carried out using the FFT code in Matlab. The decision to use log-log representations of the data came about once again because of the spread and size of the data sets being examined. The raw data FFT plots for both Aa and sunspot count used the entire data set. The resolution here would be high because of the number of points used. The yearly averaged Aa and sunspot FFT plots used one point per year and so do not have the same resolution as the other plots.

The final plots that were done were a plot of yearly averaged sunspot count versus time for the period 1700 to 2006 and an FFT of the same set of data. This was done to identify any longer term trends in sunspot count and to also determine if it was possible to use this large set of sunspot data as a proxy indicator for future trends in Aa.

When determining what graphical output was required to best explain any part of the data, there was a great deal of trial and error. Apart from the plots above various forms of moving average and weighted moving averages were attempted. The moving averages that were tried were 3, 10, 20 and 30 day moving averages and a Sovitzky-Golay weighted moving average. It was decided that even though the results of some of these plots eliminated the noise of the background data, they also eliminated crucial peak intensity data that it was thought would be more meaningful to include. Others have included moving averages [*Cliver et al*., 1998; *Clilverd et al.*, 2002] to identify overall trends however it was decided not to repeat this here for the reasons mentioned above.

5. Results

Several factors are considered here. The first step is the goal to identify any overall trends in the data, the second is to correlate the Aa data with the sunspot count data and determine if sunspot count data could be used as a proxy indicator of Aa, and the third aspect is then to determine if magnetic storms are actually getting stronger.

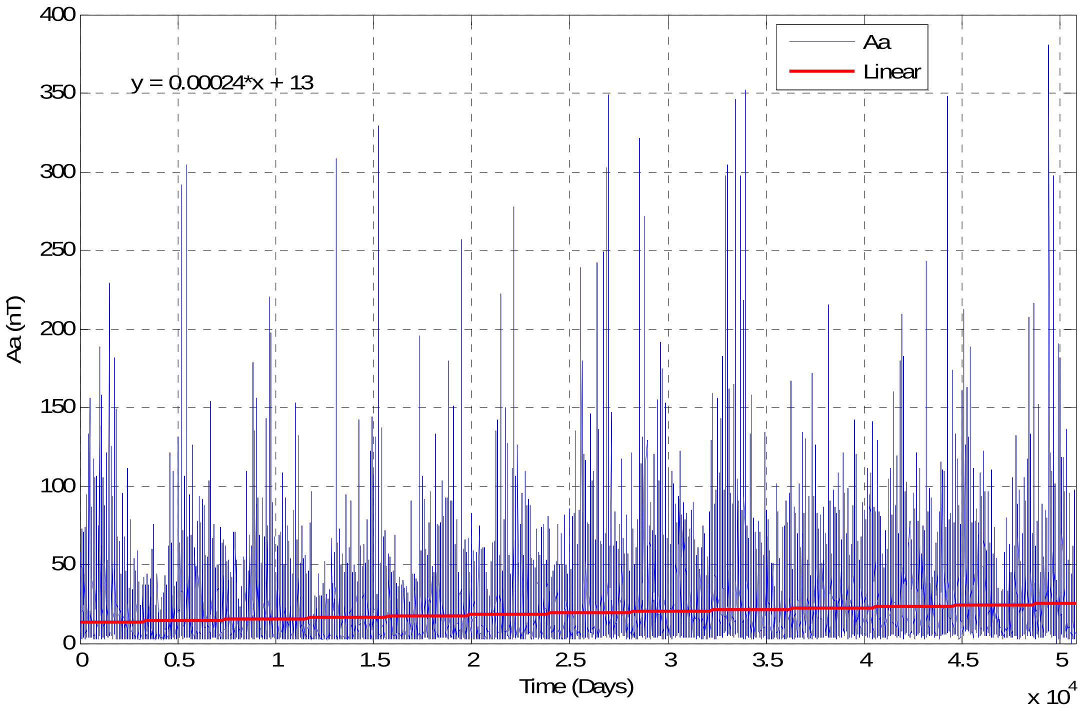

Fig. 11: Plot of Aa (nT) and Time (Days) for Period 1.1.1868 to 31.12.2006

Figure 11 is a plot of the daily Aa data for the period 1st January, 1868 to 31st December, 2006. Some periodicity can be noted however because of the size of the data set the temporal resolution when plotted like this means that some fine details at lower values of Aa may be obscured. The large peaks indicate extreme geomagnetic storms and their occurrence closely follows the solar maxima.

Inspection by eye suggests that the overall average Aa index appears to increase with time. A linear regression trend line simply fitted across all the data is shown. Such an increasing trend in Aa has been previously reported by other researchers [*Feynmann and Crooker*, 1978; *Cliver et al*, 1998]. The value for the slope of the trend line is only 2.4 x 10^{-4} nT/day (i.e. 8.8 x 10^{-2} nT/year) and even though it is increasing, this is still quite a small rate of increase.

Figure 12 shows a plot of the daily sunspot count for the period 1st January, 1868 to 31st December, 2006. The approximately 11 year solar cycles are clearly evident here. Both linear and cubic trend lines have been included so as to determine if there is indeed an increasing trend in the sunspot count value and if there are any other inherent cyclic properties of the data set. There appears to be an increase in the value of sunspot count over time however this is a very small trend. The slope of the linear trend line is 8.4 x 10^{-4} nT/day indicates a very small increase over the time period in question.

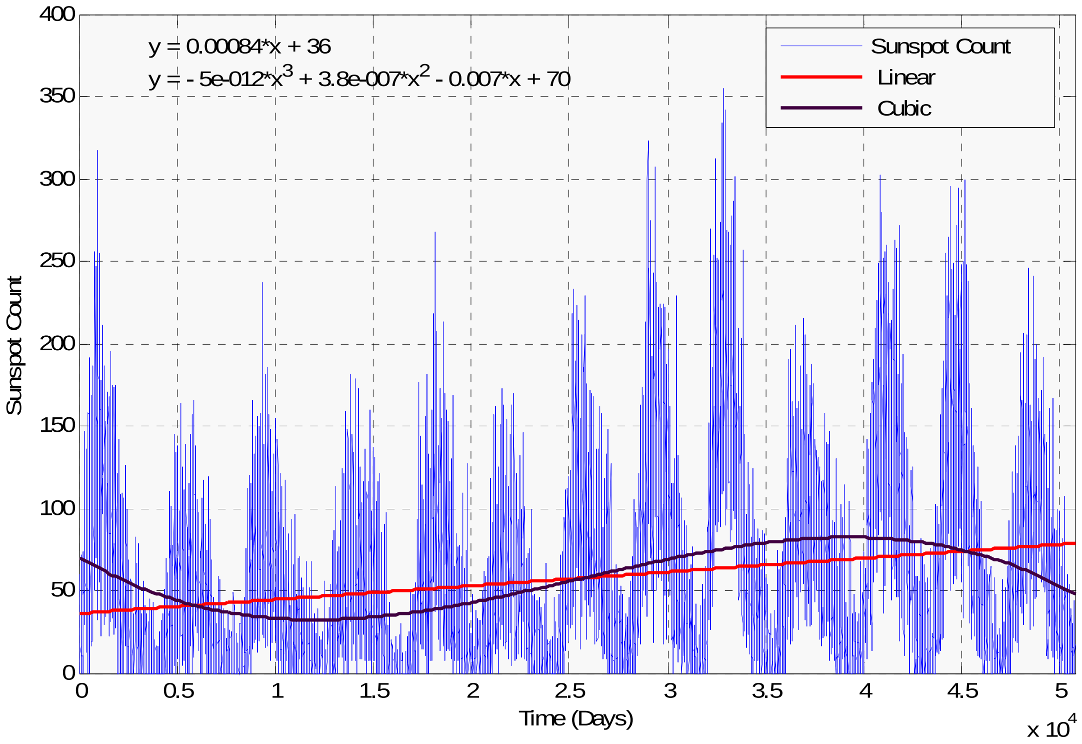

Fig. 12: Plot of Sunspot Count and Time (Days) for period 1.1.1868 to 31.12.2006

There are other features in this plot that are worthy of note. The first is that there appears to be a background cyclic pattern behind the 11 year cycle. The cubic trend line seems to have gone through one period and the peak sunspot values appear to follow a sinusoidal pattern. This pattern will be considered again when looking at the longer-term sunspot count data. The other feature to note is that there appears to be a correlation between the number of sunspots detected and the length of the solar cycle. The use of sunspot data in the current exercise was to identify correlation between Aa values and the solar cycle not for a detailed study of sunspot data, however the difference between short, squat cycles and tall, slender ones seems obvious. An example of this are the two cycles from approximately 3.2 to 4.0 x 10^4 days. The first cycle (tall and narrow) appears to be about 3000 days long while the second cycle (short and wide) appears to be about 5000 days. This is possibly something for others to further investigate.

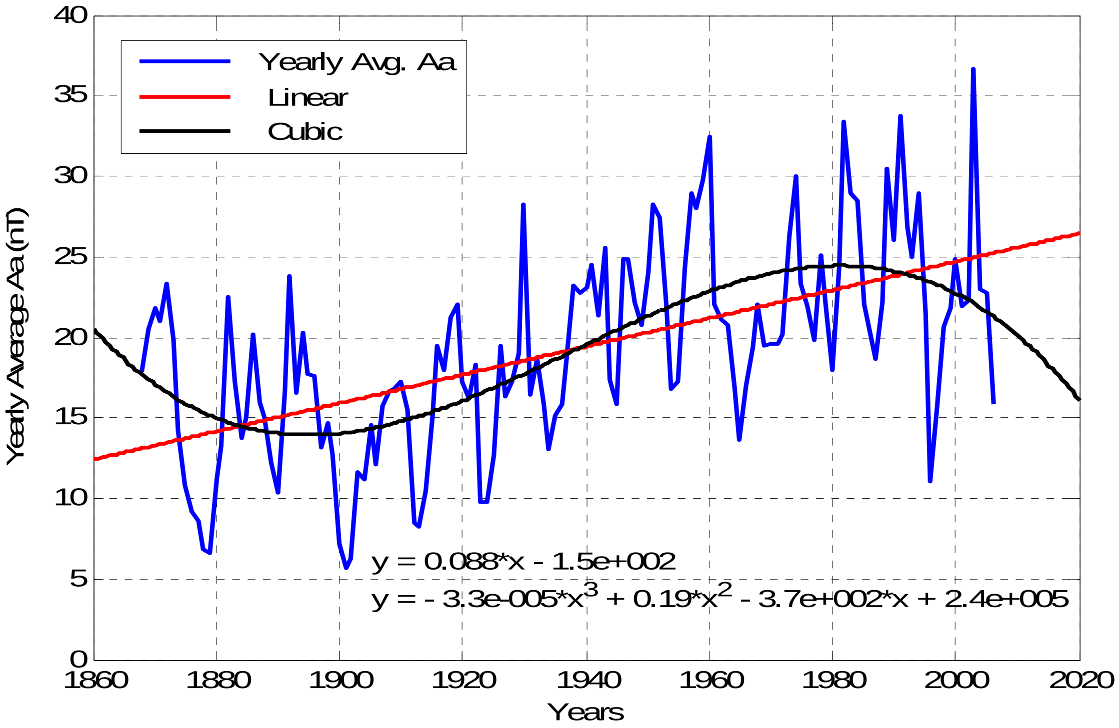

Fig. 13: Plot of Yearly Average Aa (nT) and Years for Period 1868 to 2006.

Figure 13 shows a plot of yearly averaged Aa measurements and time, in years. Again, linear and cubic regression lines have been added. These data indicate an upward trend in the value of Aa. It also shows a cyclic trend which would be because of the close correlation of the Aa index with the sunspot count and thus the approximately 11 year solar cycle.

Figure 14 shows a plot of yearly averaged sunspot count and time, in years. The solar cycles are clearly evident, as is the apparent cyclic nature of sunspot count during this particular time frame. A comparison of figures 13 and 14 show very close correlation, with peaks and troughs occurring at almost the same time. This result indicates that Aa closely follows sunspot count and so sunspot count could be used as a proxy measure for Aa.

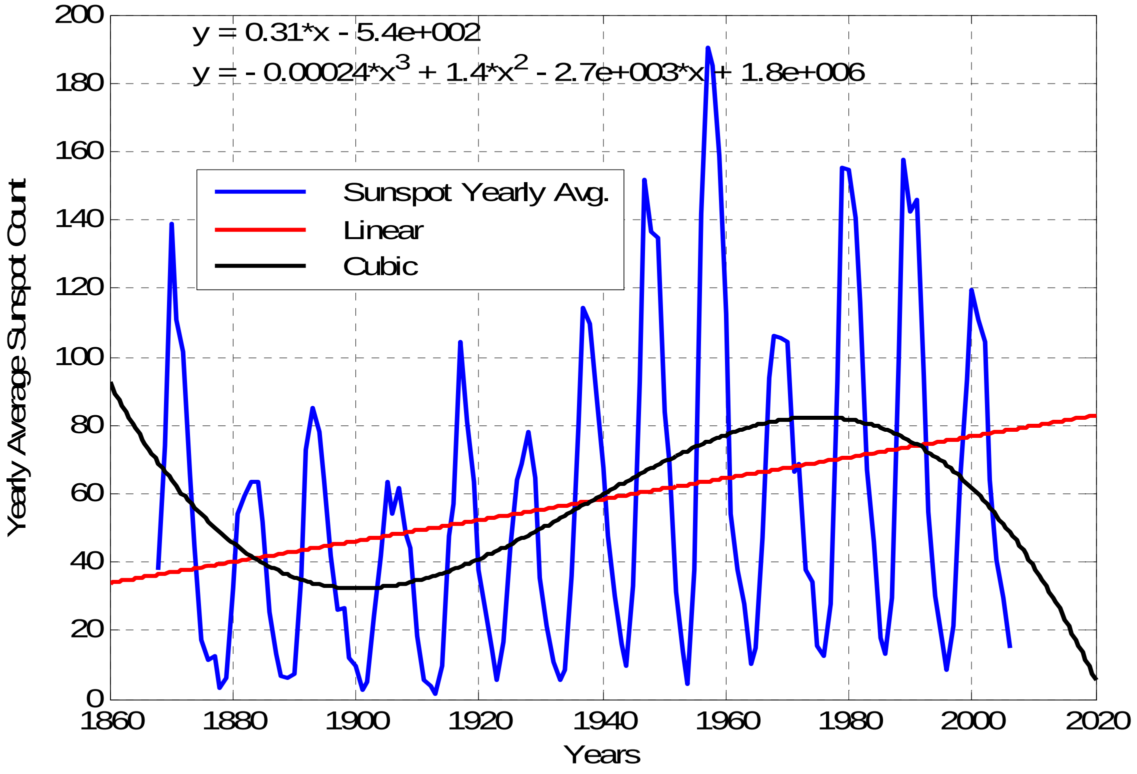

Fig. 14: Plot of Yearly Average Sunspot Count and Years for Period 1868 to 2006.

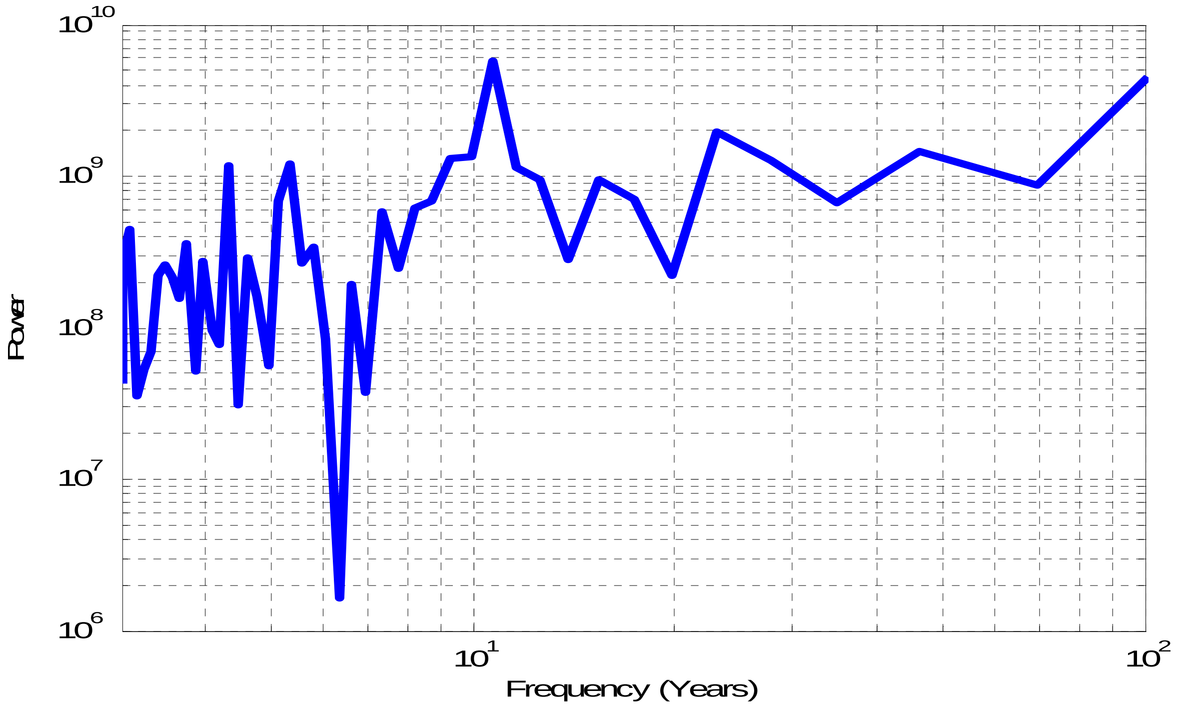

Fig. 15: Log-Log Plot of FFT Power Spectrum and Frequency (Years) for Aa Data

Figure 15 is a log-log plot of the FFT power spectrum and frequency in years of Aa data for the period 1 January, 1868 to 31 December, 2006. The plot shows peaks at approximately 5.3, 11 and 22 years. The strong peak at 11 years indicates the frequency of the solar cycle. The other two peaks are much smaller and indicate sub-harmonic and harmonic effects.

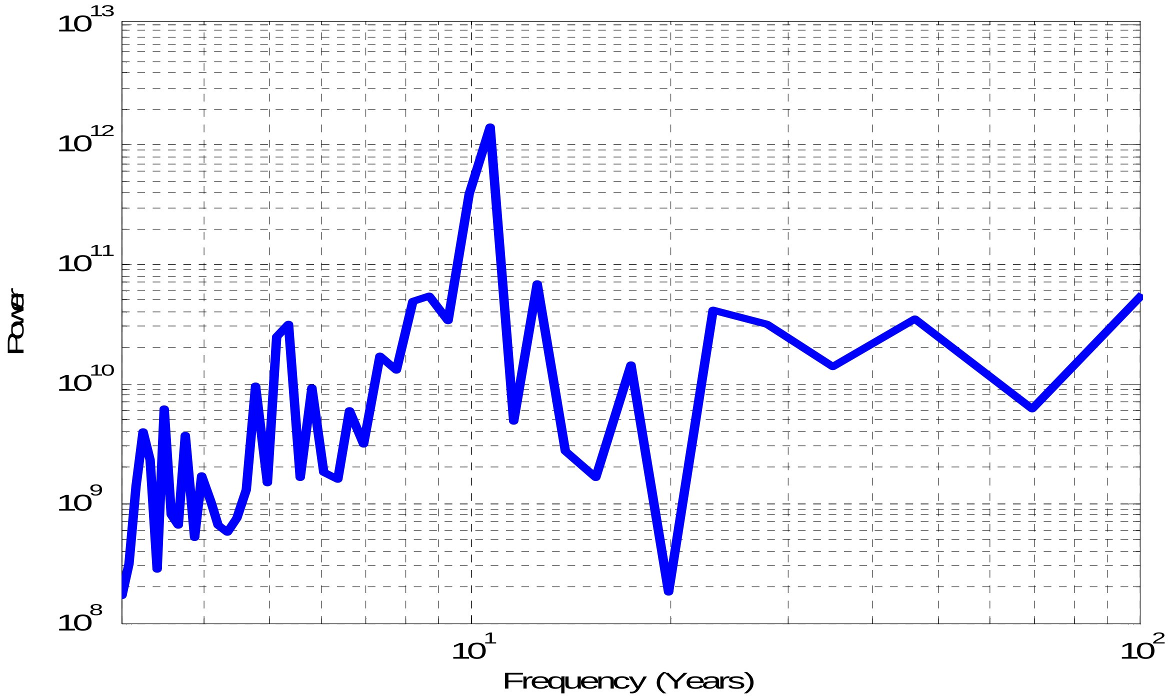

Fig. 16: Log-Log Plot of FFT Power Spectrum and Frequency (Years) for Sunspot Count Data

Figure 16 shows a log-log plot of FFT and frequency, in years, for sunspot count data for the period 1 January, 1868 to 31 December, 2006. The strong peak occurs at the 11 year solar cycle frequency. There are smaller peaks at around 5.3, 12.5 and 22 years. The peak at 12.5 years could indicate that solar cycles aren't exactly 11 years in duration and so there is some spread of sunspot numbers. The peaks at 5.3 and 22 years are sub-harmonic and harmonic effects in the data.

A comparison of Figures 15 and 16 indicate that, as determined earlier, Aa closely follows solar activity as measured by the sunspot count. The stronger sunspot count peaks indicate that they are the driver in this process and the Aa values are the driven response. This is the result that was to be expected.

Figure 17 shows a plot of yearly average sunspot count and years for the period 1700 to 2006. This plot clearly shows the solar cycles for the period in question. It also shows what was noted earlier regarding the number of sunspots and the length of the solar cycle. The linear trend is superimposed on three longer term cycles. The maximum peak occurs around 1957 when there was an extremely active solar maximum.

Figure 18 is a log-log plot of the FFT power spectrum and frequency, in years, of yearly averaged sunspot count data for the period 1700 to 2006. The main peak is found at the 11 year mark, indicating the frequency of the solar cycle. Subsequent peaks are also found at around 22, 29, 50 and 100 years. These are once again harmonics and sub-harmonics. The peaks at 50 and 100 years therefore indicate a 100 year cycle with a 50 year sub harmonic.

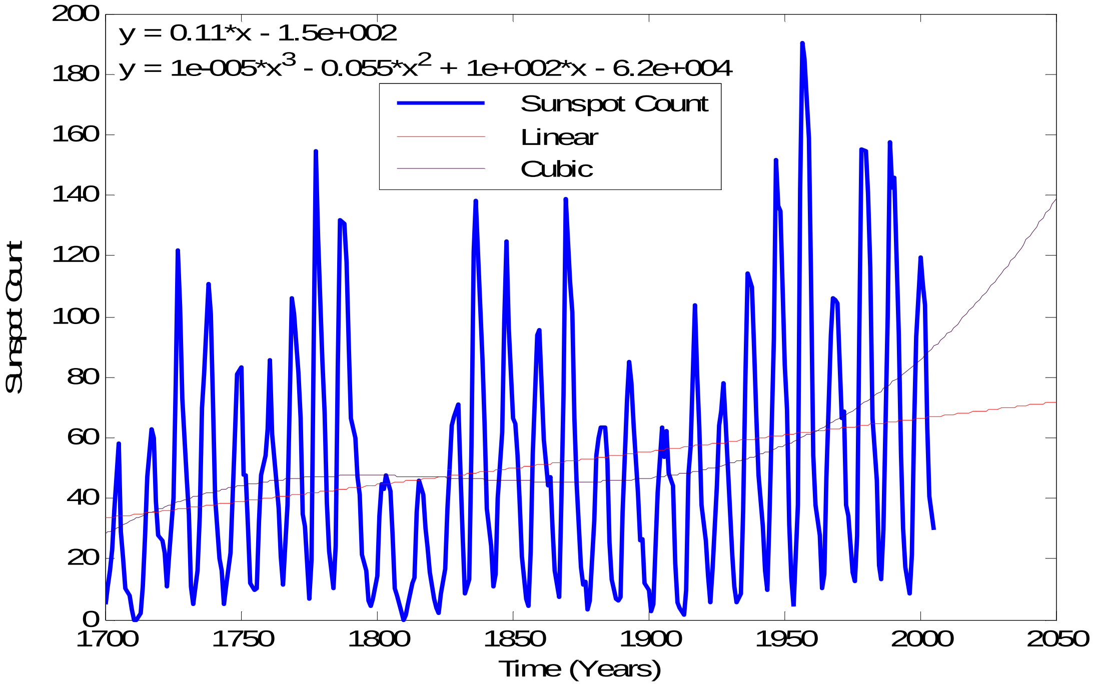

Fig. 17: Plot of Yearly Average Sunspot Count and Years for Period 1700 to 2006.

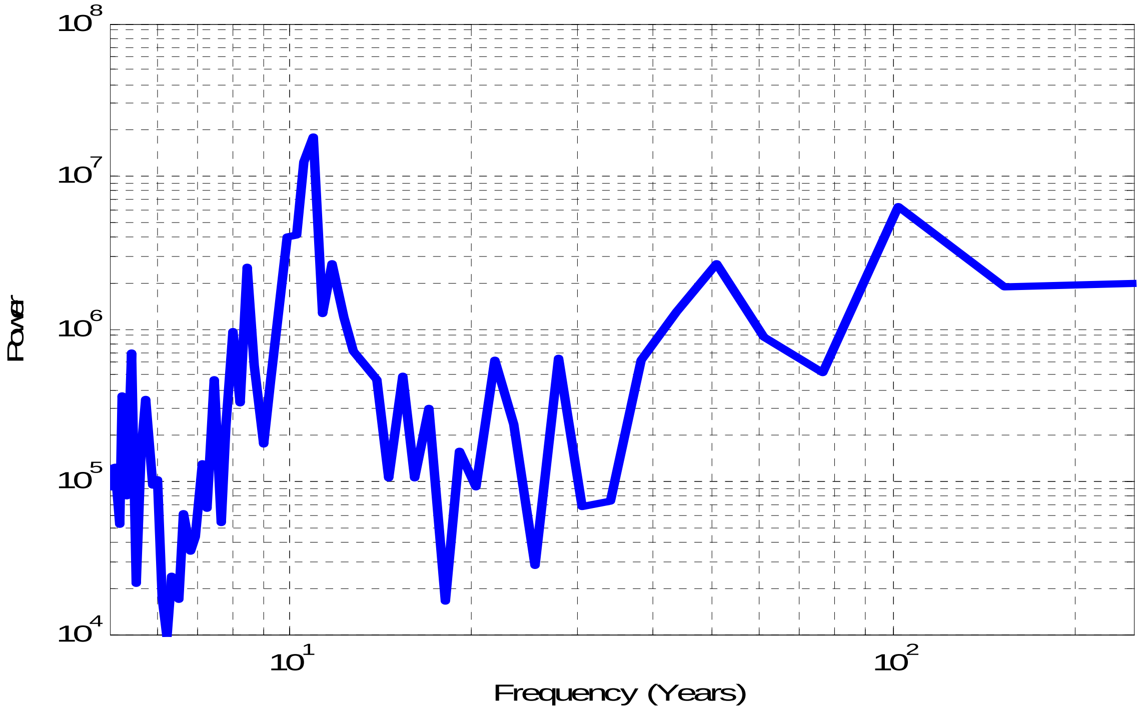

Fig. 18: Log-Log Plot of FFT Power Spectrum and Frequency (Years) for Yearly Averaged Sunspot Count Data for Period 1700 to 2006.

Date	Aa (nT)	Max. aa (nT)
20/11/1882	304	658
31/10/1903	308	658
25/09/1909	329	526
18/09/1941	349	656
28/03/1946	321	698
8/07/1958	304	698
15/07/1959	346	568
13/11/1960	352	715
13/03/1989	348	715
11/05/2003	381	405

Table 1: Magnetic Storms Occurring in the Period 1.1.1868 to 31.12.2006 with Aa > 300 nT.

Table 1 shows the magnetic storms that exceeded an Aa value of 300nT during the past 139 years. The average intensity of these storms is 334.2nT with a standard deviation of 25nT. This table shows that superstorms can occur at any time and that individually they are not getting any larger.

The Halloween Storm of 2003 – An Example

Starting around 19 October and lasting until about 4 November 2003, an unusual increase in high-energy particle fluxes occurred in near-Earth space. The increase in the number and intensity of X-ray flares, energetic particle flux peaks, and extreme ultraviolet (EUV) radiation events was a consequence of several coronal mass ejections (CMEs) and solar flares that occurred during this period. These were associated with three giant sunspot groups, each larger than the planet Jupiter. The effects on Earth were many. Radio blackouts disrupted communications. Solar protons penetrated Earth's upper atmosphere, exposing astronauts and some air travelers to radiation doses equal to a medical chest X-ray. To get an idea of how these solar events compare with other large solar events, consider that auroras from these events extended farther toward the equator than usual, appearing in Florida, Texas, Australia, and many other places where they are seldom seen. In California, where smoke from wildfires dimmed the Sun enough to look straight at it, the huge blotches on the Sun startled casual sky watchers. One of the spots, the one named NOAA 486 (see Figure 19), was the largest in 13 years. These sunspots unleashed 11 X-class flares in only 14 days, equaling the total number observed during the previous 12 month period [*Barbieri and Mahmot,* 2003].

As an indication of the type of environment that was generated during this time a brief explanation of flare ranking is in order. Researchers rank solar flares according to their X-ray power output. C flares are the weakest. M flares are moderately strong. X flares are the most powerful. Each category has subdivisions: X1, X2, X3, and so on. X-ray flare classification uses a log scale. That is, an X-class flare is 10 times the strength of a correspondingly ranked M-class flare; for example, an X1 flare has 10 times the peak power of an M1 flare. A typical X flare registers X1 or X2. On 4 November, sunspot NOAA 486 unleashed an X28 flare, the most powerful ever recorded at that time. In 1989 a flare about half that strong caused a widespread power blackout in Quebec (the

March 1989 storm). Luckily this November flare was aimed away from Earth and so its effects were only slight [*Barbieri and Mahmot*, 2003].

The effects on NASA spacecraft are detailed in the Table in Appendix 2. This table is taken from Barbieri and Mahmot [2003] and shows the effects on spacecraft and instrumentation of the storm. It must be remembered that this is only NASA's fleet and does not include spacecraft owned by different countries, commercial operators, and other space related organisations. According to Barbieri and Mahmot, 59% of spacecraft and 18% of the instrument groups experienced some effect from this activity [*Barbieri and Mahmot*, 2003]

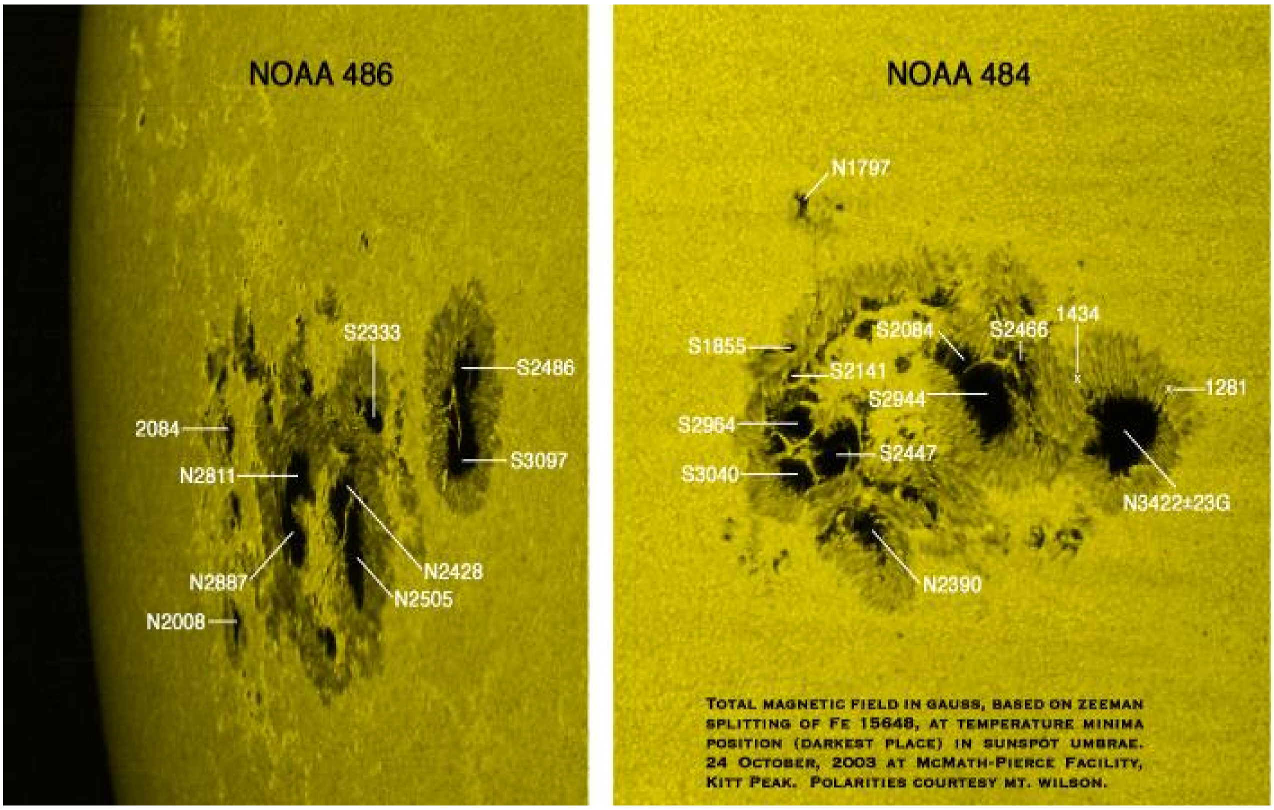

TOTAL MAGNETIC FIELD IN GAUSS, BASED ON ZEEMAN SPLITTING OF FE 15648, AT TEMPERATURE MINIMA POSITION (DARKEST PLACE) IN SUNSPOT UMBRAE. 24 OCTOBER, 2003 AT MCMATH-PIERCE FACILITY, KITT PEAK. POLARITIES COURTESY MT. WILSON.

Fig.19: Shows a Photograph of Sunspot NOAA486 and NOAA 484. (Photo Courtesy NOAO/AURA/NSF. Picture by Dr Bill Livingston.)

Table 1 above shows the ten storms that exceeded an Aa value of 300 nT during the past 139 years. A point to note is that the Halloween Storm only missed out on being a member of this group by 2 nT. The Aa reading for 29th October, 2003 was 298 nT with a maximum aa reading of 715 nT. Figure 7 above shows a plot of the hourly Dst index against time in hours of the Halloween Storm period in late October and early November 2003. This plot shows the intensity of the storm and the arrival of a second shockwave as the initial storm is in the recovery phase.

6. Discussion

The results of this project indicate that there has been a linear increase in aa as measured using the Aa index for the period 1 January, 1868 to 31 December, 2006. This is evidenced in Figures 11 and 13, both of which show the increase. The increase is relatively small considering the period of time over which this data set runs however it is evident. The lines of best fit were added to see if indeed there had been an increase in Aa over time. The cubic line was added to see if the data followed this type of curve. It should also be noted that the peak intensities of Aa do not follow exactly the peaks of the sunspot count data. A large proportion of the higher intensity Aa results occur in the declining phase of the solar cycle. This has been established previously. The problem lies with the high intensity peaks that don't conform to this rule and occur at other times. These storms make prediction very difficult especially if they occur during solar minimum when they are least expected.

The periodicity noted in both of these figures is directly related to the periodicity of the sunspot count data as shown in Figures 12 and 14. The approximate 11 year solar cycle is clearly noted and the intensity of the Aa results seems to follow this cycle almost exactly. There is however a background cycle apparent in the sunspot figures and the Aa results also follow this cyclic pattern. The intensity of the Aa results mirrors the sunspot count numbers. That is when sunspot numbers are high so is the Aa result. When sunspot numbers are lower so is the relative intensity of Aa. This is to be expected as the activity of the sun is mirrored in sunspot counts and the more active the sun, the more sunspots, and the greater the chance of solar flares and CMEs sending charged particles toward Earth and increasing the velocity of the solar wind, thus causing a greater incidence of magnetic storms.

The FFT plots, Figures 15 and 16, are also very similar. The y axis of both plots is the power of the signal and it is an arbitrary figure. The frequency is not and it is clearly visible that there is a driving effect and that there is a driven effect. The Aa results are the driven effect. Solar activity is what drives the number of sunspots and so it is this activity which can greatly affect the Earth's magnetosphere and thus cause geomagnetic storms. The solar cycle frequency of 11 years is clearly visible in both plots. There are other smaller peaks visible and in the case of both plots there is a peak at around 22years. This effect is due to the overall 22 year magnetic cycle of the Sun. Other smaller peaks are possibly harmonic effects. The purpose of doing FFT analysis of the data was to determine if there is any inherent background cyclic behaviour that is not visible in the other plots. This was not the case and the cyclic behaviour noted in the normal plots did not translate into the FFT.

Figure 17 shows the 306 year plot of sunspot numbers. Another part of this project was to investigate the long term sunspot count and determine if it could be used as a proxy measure of aa. The close correlation of sunspot number and Aa as determined in other results would tend to indicate that the sunspot count could be used as a proxy measure for aa. The FFT plot of this data set, Figure 18, shows the 11 year solar cycle frequency. It also shows some strong peaks at around 50 years and around 100years. These peaks are only less than one order of magnitude below the 11 year level and so are significant when looking at longer sunspot cycles.

The main aim of this project was to determine if magnetic storms are actually getting stronger. Table 1 shows a list of magnetic storms that have occurred during the 139 year data period that had Aa values greater than 300nT. These would be classed as super storms. The reasoning behind looking at these 'big storms' was to see if there was any noticeable increase in 'big storm' intensity over time. This was not the case. The intensity of individual storms does not appear to have increased over time.

With an increasing sunspot count and an increasing Aa value over the last 139 years, the strength of magnetic storms in general must be increasing. The trend in Aa can be seen by eye from the plots of the daily data, as can the sunspot count. The number of storms has increased [*Clilverd et al*., 1998] and with the increase in aa and sunspot count over time, there is a strong probability that magnetic storms are getting stronger, albeit by very small amounts.

The main reason for determining whether geomagnetic storms are getting stronger is the effect that they have on man-made infrastructure. As mentioned earlier, space weather can affect spacecraft, aircraft, radio frequency propagation, power generation and transportation systems, oil and gas pipeline systems and humans. The increasing vulnerability of sophisticated systems to space weather effects is becoming a concern to a large number of people. If magnetic storms are getting stronger, then engineers need to be able to accommodate possible space weather effects into design processes. In a paper entitled 'Single Event Effects in Avionics', Boeing's Eugene Normand discusses the problem of single event upsets (SEUs) in aircraft electronics. The problems encountered were real and the measured inflight SEU rate correlated with atmospheric neutron flux. This paper was written in the mid 1990s. So the effects on more sophisticated electronics would be greater now than they were then. Problems with spacecraft have also increased as have concerns over Earth based infrastructure. Insurance companies that insure spacecraft, both launchers and payloads, have a vested interest in space weather and its prediction. As discussed earlier trillions and trillions of dollars are invested in vulnerable infrastructure items that need to be covered by insurance. If insurers are aware of space weather events then they can better evaluate their risks.

In some interesting recent news a researcher, Leif Svalgaard, in an article entitled 'Calibrating the Sunspot Number using "the Magnetic Needle"', has said that a 9.8% increase in the east-ward component of the geomagnetic field as measured at Hobart during the past 166 years, was caused by a 9% decrease in the Earth's main dipole field over the same time period. He states that the increase in ionospheric conductivity caused by the decreasing field would have caused the increase in rY. [Svalgaard, 2007]

7. Conclusion

The aa index has shown an increase over the past 139 years. This result confirms earlier work carried out by other researchers [*Feynman and Crooker*, 1978 and *Cliver et al*, 1998 as cited in *Clilverd et al,*. 2002]. The sunspot count data has also shown an increase over the same period of time. The aa data and sunspot data show excellent correlation and so over time sunspot data can be used as a proxy measure for aa. The number of magnetic storms has increased [*Clilverd et al.,* 1998] indicating an increase in solar variability. An increase in solar variability combined with increasing numbers of sunspots would therefore indicate that there would be an increase in strength of magnetic storms. Therefore based on the results and analysis of the data, the strength of magnetic storms does seem to be increasing, however, at a very small rate.

The basis for the investigation into the strength of magnetic storms relates to the effects that space weather in general and geomagnetic storms in particular can have on man-made infrastructure. As discussed earlier space weather can affect spacecraft, aircraft, radio frequency propagation, power generation and transportation systems, oil and gas pipeline systems and humans. There is an ongoing need to develop more robust systems that are exposed to space weather and to better protect the humans that are exposed to space weather. There is also a need to continue developing sophisticated measuring and forecasting systems so that everyone can be prepared for the next big storm.

8. References

aa, Kpa Indices. (2007). Retrieved 6 April, 2007 from http://isgi.cetp.ipsl.fr/lesdonne.htm

Australian Geomagnetism Report. (1999). Retrieved 11 June, 2007 from
http://www.intermagnet.org/yearbooks/AGR99part1.pdf

Barbieri, L. P., and R. E. Mahmot (2004), October--November 2003's space weather and operations lessons learned, *Space Weather*, 2, S09002, doi:10.1029/2004SW000064

Butterfly Diagram.(n.d.). Retrieved 5 June, 2007, from http://solar.physics.montana.edu/YPOP/Spotlight/Magnetic/Images/butterfly.jpg

Campbell, W., *Introduction to Geomagnetic Fields*, 1997, Cambridge University Press, Cambridge, UK.

Clilverd, M.A., T. D. G. Clark, E. Clarke, H. Risbeth, and T. Ulich. The causes of long-term change in the *aa* index, *J. Geophys. Res.*, 107(A12)1441, doi: 10.1029/2001JA000501, 2002.

Clilverd, M.A., E. Clarke, T. Ulich, J. Linthe and H. Risbeth. Reconstructing the long-term aa index, *J. Geophys. Res.*, 110, A07205, doi: 10.1029/2004JA010762, 2005.

Cliver, E.W., V. Boriakoff and J. Feynman. Solar variability and climate change: Geomagnetic aa index and global surface temperature, *Geophysical Research Letters.* 25 (7) pp1035-1038, 1998.

Coronal Features (2007). Retrieved 23 June, 2007 from http://solarscience.msfc.nasa.gov/feature3.shtml

Coronal Holes. (n.d.) Retrieved 6 June, 2007 from http://www.spaceweather.com/glossary/coronalholes.html

Geomagnetic Storm. 2007. Retrieved 12 May, 2007 from http://pluto.space.swri.edu/IMAGE/glossary/geomagnetic_storm.html

Hartland Observatory Monthly Magnetic Bulletin, April 2007. (2007). Retrieved 11 June 2007 from http://www.geomag.bgs.ac.uk/bulletins/had/had_apr07.pdf

Koskinen, H., E. Tanskanen, R. Pirjola, A. Pulkkinen, C. Dyer, D Rodgers, P. Cannon, J. C. Mandeville and D. Boscher. ESA Space Weather Study (ESWS). Space Weather Effects Catalogue. 2001.

Magnetosphere. (n.d.). Retrieved 23 June, 2007 from http://science.nasa.gov/ssl/pad/sppb/edu/magnetosphere/images/mag_sketch.gif

Menvielle, M. Derivation and dissemination of geomagnetic indices, *Revista Geofisica,* 48, 51-66, 1998.

NOAA Space Weather Scale for Geomagnetic Storms (2005). Retrieved 13 June 2007 from http://www.sec.noaa.gov/NOAAscales/#GeomagneticStorms

Normand, E., *Single Event Effects in Avionics.* Boeing Defense and Space Group, Seattle, WA.

Sunspot. (2007). Retrieved 21 June 2007 from http://en.wikipedia.org/wiki/Sunspot

Sunspot Numbers. (2007). Retrieved 26 April, 2007 from http://www.ngdc.noaa.gov/stp/SOLAR/ftpsunspotnumber.html

Sunspots: Modern Research. (n.d.).Retrieved 6 June, 2007, from http://www.exploratorium.edu/sunspots/research.html.

Sunspots NOAA 486/484 (2003). Retrieved 25 June, 2007 from http://www.noao.edu/image_gallery/images/d7/04700a.jpg

Svalgaard. L., Calibrating the Sunspot Number using “the Magnetic Needle”, *CAWSES News*, Vol 4, No 1, p6. 2007

The Sun's Magnetic Field Changes. (n.d.). Retrieved 6 June, 2007, from http://solar.physics.montana.edu/YPOP/Spotlight/Magnetic/cycle.html

What is a Solar Flare?(n.d.) Retrieved 6 June, 2007, from http://hesperia.gsfc.nasa.gov/sftheory/flare.htm

9. Appendices

Appendix 1: NOAA Space Weather Scale for Geomagnetic Storms

Category		**Effect**	**Physical measure**	**Average Frequency (1 cycle = 11 years)**
Scale	**Descriptor**	**Duration of event will influence severity of effects**		
Geomagnetic Storms			**Kp values* determined every 3 hours**	**Number of storm events when Kp level was met; (number of storm days)**
G 5	**Extreme**	**Power systems:** : widespread voltage control problems and protective system problems can occur, some grid systems may experience complete collapse or blackouts. Transformers may experience damage. **Spacecraft operations:** may experience extensive surface charging, problems with orientation, uplink/downlink and tracking satellites. **Other systems:** pipeline currents can reach hundreds of amps, HF (high frequency) radio propagation may be impossible in many areas for one to two days, satellite navigation may be degraded for days, low-frequency radio navigation can be out for hours, and aurora has been seen as low as Florida and southern Texas (typically 40° geomagnetic lat.)**.	Kp = 9	4 per cycle (4 days per cycle)
G 4	**Severe**	**Power systems:** possible widespread voltage control problems and some protective systems will mistakenly trip out	Kp = 8, including a 9-	100 per cycle (60 days per cycle)

		key assets from the grid. **Spacecraft operations:** may experience surface charging and tracking problems, corrections may be needed for orientation problems. **Other systems:** induced pipeline currents affect preventive measures, HF radio propagation sporadic, satellite navigation degraded for hours, low-frequency radio navigation disrupted, and aurora has been seen as low as Alabama and northern California (typically 45° geomagnetic lat.)**.		
G 3	**Strong**	**Power systems:** voltage corrections may be required, false alarms triggered on some protection devices. **Spacecraft operations:** surface charging may occur on satellite components, drag may increase on low-Earth-orbit satellites, and corrections may be needed for orientation problems. **Other systems:** intermittent satellite navigation and low-frequency radio navigation problems may occur, HF radio may be intermittent, and aurora has been seen as low as Illinois and Oregon (typically 50° geomagnetic lat.)**.	Kp = 7	200 per cycle (130 days per cycle)
G 2	**Moderate**	**Power systems:** high-latitude power systems may experience voltage alarms, long-duration storms may cause transformer damage. **Spacecraft operations:** corrective actions to orientation may be required by ground control; possible changes in drag affect orbit predictions. **Other systems:** HF radio propagation can fade at higher latitudes, and aurora has been seen as low as New York and Idaho (typically 55° geomagnetic lat.)**.	Kp = 6	600 per cycle (360 days per cycle)
G 1	**Minor**	**Power systems:** weak power grid fluctuations can occur. **Spacecraft operations:** minor impact on satellite operations possible. **Other systems:** migratory animals are affected at this and higher levels; aurora is commonly visible at high latitudes (northern Michigan and Maine)**.	Kp = 5	1700 per cycle (900 days per cycle)

The K-index used to generate these messages are derived in real-time from the Boulder NOAA Magnetometer. The Boulder K-index, in most cases, approximates the Planetary Kp-index referenced in the NOAA Space Weather Scales. The Planetary Kp-index is not available in real-time.
** For specific locations around the globe, use geomagnetic latitude to determine likely sightings

Appendix 2: Space Weather Effect Summary for Spacecraft and Instrument Related Impacts during Halloween Storm of 2003

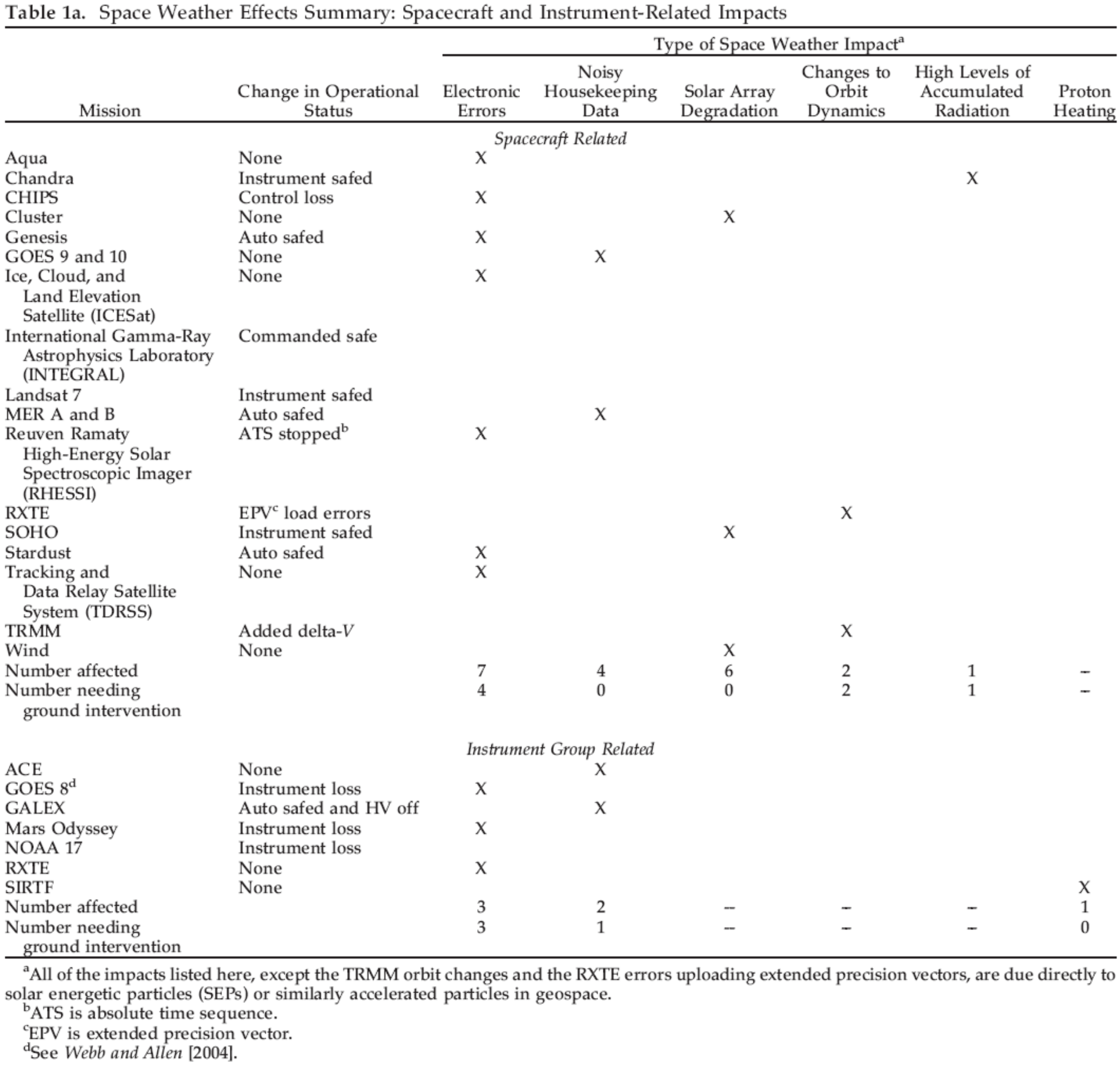

Table 1a. Space Weather Effects Summary: Spacecraft and Instrument-Related Impacts

Mission	Change in Operational Status	Type of Space Weather Impact[a]					
		Electronic Errors	Noisy Housekeeping Data	Solar Array Degradation	Changes to Orbit Dynamics	High Levels of Accumulated Radiation	Proton Heating
Spacecraft Related							
Aqua	None	X					
Chandra	Instrument safed					X	
CHIPS	Control loss	X					
Cluster	None			X			
Genesis	Auto safed	X					
GOES 9 and 10	None		X				
Ice, Cloud, and Land Elevation Satellite (ICESat)	None	X					
International Gamma-Ray Astrophysics Laboratory (INTEGRAL)	Commanded safe						
Landsat 7	Instrument safed						
MER A and B	Auto safed		X				
Reuven Ramaty High-Energy Solar Spectroscopic Imager (RHESSI)	ATS stopped[b]	X					
RXTE	EPV[c] load errors				X		
SOHO	Instrument safed			X			
Stardust	Auto safed	X					
Tracking and Data Relay Satellite System (TDRSS)	None	X					
TRMM	Added delta-V				X		
Wind	None			X			
Number affected		7	4	6	2	1	–
Number needing ground intervention		4	0	0	2	1	–
Instrument Group Related							
ACE	None		X				
GOES 8[d]	Instrument loss	X					
GALEX	Auto safed and HV off		X				
Mars Odyssey	Instrument loss	X					
NOAA 17	Instrument loss						
RXTE	None	X					
SIRTF	None						X
Number affected		3	2	–	–	–	1
Number needing ground intervention		3	1	–	–	–	0

[a] All of the impacts listed here, except the TRMM orbit changes and the RXTE errors uploading extended precision vectors, are due directly to solar energetic particles (SEPs) or similarly accelerated particles in geospace.
[b] ATS is absolute time sequence.
[c] EPV is extended precision vector.
[d] See *Webb and Allen* [2004].

from: Barbieri, L. P., and R. E. Mahmot (2004), October--November 2003’s space weather and operations lessons learned, Space Weather, 2, S09002, doi:10.1029/2004SW000064.